TKK Dissertations 100
Espoo 2007

SENSORLESS CONTROL OF AC DRIVES EQUIPPED WITH AN INVERTER OUTPUT FILTER

Doctoral Dissertation

Janne Salomäki

Helsinki University of Technology
Department of Electrical and Communications Engineering
Power Electronics Laboratory

TKK Dissertations 100
Espoo 2007

SENSORLESS CONTROL OF AC DRIVES EQUIPPED WITH AN INVERTER OUTPUT FILTER

Doctoral Dissertation

Janne Salomäki

Dissertation for the degree of Doctor of Science in Technology to be presented with due permission of the Department of Electrical and Communications Engineering for public examination and debate in Auditorium S4 at Helsinki University of Technology (Espoo, Finland) on the 21st of December, 2007, at 12 noon.

Helsinki University of Technology
Department of Electrical and Communications Engineering
Power Electronics Laboratory

Teknillinen korkeakoulu
Sähkö- ja tietoliikennetekniikan osasto
Tehoelektroniikan laboratorio

Distribution:
Helsinki University of Technology
Department of Electrical and Communications Engineering
Power Electronics Laboratory
P.O. Box 3000
FI - 02015 TKK
FINLAND
URL: http://powerelectronics.tkk.fi/
Tel. +358-9-451 2431
Fax +358-9-451 2432
E-mail: janne.salomaki@konecranes.com

ISBN 978-951-22-9129-8
ISBN 978-951-22-9130-4 (PDF)
ISSN 1795-2239
ISSN 1795-4584 (PDF)
URL: http://lib.tkk.fi/Diss/2007/isbn9789512291304/

TKK-DISS-2400

Multiprint Oy
Espoo 2007

ABSTRACT OF DOCTORAL DISSERTATION	HELSINKI UNIVERSITY OF TECHNOLOGY P. O. BOX 1000, FI-02015 TKK http://www.tkk.fi

Author Janne Salomäki

Name of the dissertation

Sensorless Control of AC Drives Equipped With an Inverter Output Filter

Manuscript submitted 2.7.2007	Manuscript revised 1.11.2007
Date of the defence 21.12.2007	
☐ Monograph	☒ Article dissertation (summary + original articles)
Department	Department of Electrical and Communications Engineering
Laboratory	Power Electronics Laboratory
Field of research	Electrical engineering
Opponent(s)	Prof. Ralph Kennel
Supervisor	Prof. Jorma Luomi
Instructor	

Abstract

In this thesis, new sensorless control methods are developed for AC motor drives equipped with an inverter output filter. A three-phase LC filter with a cut-off frequency well below the switching frequency of the inverter enables nearly sinusoidal supply voltage for the motor. Induction motors and permanent magnet synchronous motors are typically connected directly to the frequency converter. In some applications, however, it is necessary to add a filter between the inverter and the motor in order to mitigate the harmful effects of the pulse-width modulated (PWM) voltage. The control methods proposed in this thesis take an LC filter into account. Besides the conventional stator current control, two nested control loops are added to control the stator voltage and the inverter output current. A full-order observer of the motor dynamics is augmented with the filter dynamics. The observer enables the vector control without any additional current or voltage measurements. Furthermore, the drive should preferably work without a speed sensor. A speed adaptation mechanism is added to the observer enabling the speed-sensorless operation. The selection of the observer gain and adaptation parameters is based on the linearization analysis of the system. Speed-sensorless control methods are known to have stability problems at low speeds. Similar problems occur when the inverter output filter is used. To enhance the stability at low speeds, the speed-adaptive observer is augmented with a high-frequency signal injection method for permanent magnet synchronous motor drives equipped with an LC filter. The signal injection enables sustained operation even at zero speed under load changes. Field-weakening methods are also developed for AC motor drives equipped with an inverter output filter. Computer simulations and experiments validate the performance of the proposed control methods in wide speed and load ranges. In addition, the influence of the inverter output filter on the selection of the PWM method is investigated. If a common-mode filter is used, discontinuous PWM methods may cause excessive vibration in the common-mode current. A conventional space vector PWM is suitable method, because it does not generate significant harmonics near the resonance frequency of the common-mode filter. The cost-effective filter design is also considered. Filtering requirements and the limitation caused by the vector control are taken into account in the filter design.

Keywords Inverter output filter, induction motor, permanent magnet synchronous motor, sensorless control

ISBN (printed) 978-951-22-9129-8	ISSN (printed) 1795-2239
ISBN (pdf) 978-951-22-9130-4	ISSN (pdf) 1795-4584
Language English	Number of pages 143
Publisher Multiprint Oy	
Print distribution Power Electronics Laboratory	

☒ The dissertation can be read at http://lib.tkk.fi/Diss/2007/isbn9789512291304/

VÄITÖSKIRJAN TIIVISTELMÄ	TEKNILLINEN KORKEAKOULU PL 1000, 02015 TKK http://www.tkk.fi

Tekijä Janne Salomäki

Väitöskirjan nimi

Taajuusmuuttajan lähtösuodattimella varustettujen vaihtovirtakäyttöjen anturiton ohjaus

Käsikirjoituksen päivämäärä 2.7.2007	Korjatun käsikirjoituksen päivämäärä 1.11.2007
Väitöstilaisuuden ajankohta 21.12.2007	
☐ Monografia	☒ Yhdistelmäväitöskirja (yhteenveto + erillisartikkelit)

Osasto	Sähkö- ja tietoliikennetekniikan osasto
Laboratorio	Tehoelektroniikan laboratorio
Tutkimusala	Sähkötekniikka
Vastaväittäjä(t)	Prof. Ralph Kennel
Työn valvoja	Prof. Jorma Luomi
Työn ohjaaja	

Tiivistelmä

Väitöskirjassa kehitetään uusia anturittomia säätömenetelmiä vaihtovirtamoottoreille, kun taajuusmuuttajan lähtöjännitettä parannetaan suodattimella. Kolmivaiheinen LC-suodatin, jonka rajataajuus on pienempi kuin taajuusmuuttajan kytkentätaajuus, mahdollistaa lähes sinimuotoisen moottorin syöttöjännitteen. Oikosulkumoottorit ja kestomagneettitahtimoottorit kytketään tavallisesti suoraan taajuusmuuttajan lähtöön. Joissakin tapauksissa on kuitenkin välttämätöntä käyttää suodatinta taajuusmuuttajan ja moottorin välissä, jotta päästäisiin eroon pulssinleveysmoduloidun jännitteen aiheuttamista haitallisista ilmiöistä. Väitöskirjassa ehdotetut säätömenetelmät ottavat LC-suodattimen huomioon. Staattorin virtasäätöön lisätään kaksi sisäkkäistä säätösilmukkaa staattorin jännitteelle ja vaihtosuuntaajan lähtövirralle. Moottorin täyden kertaluvun tilahavaitsijaan lisätään suodattimen dynaaminen malli, jolloin vektorisäätö on mahdollista ilman lisämittauksia järjestelmän virroista tai jännitteistä. Käytön pitäisi toimia myös ilman nopeusanturia. Kun tilahavaitsijaan lisätään nopeuden adaptointi, liikeanturiton säätö on mahdollista. Tilahavaitsijan ja adaptoinnin parametrit voidaan valita käyttäen apuna järjestelmän linearisointianalyysiä. Nopeusanturittomilla säätömenetelmillä on tunnetusti stabiiliusongelmia pienillä nopeuksilla. Samanlaisia ongelmia esiintyy myös lähtösuodattimella varustetuissa käytöissä. Kestomagneettitahtimoottoreiden tapauksessa adaptointimekanismiin liitetään suurtaajuussignaali-injektiomenetelmä, joka mahdollistaa stabiilin toiminnan jopa nollanopeudella kuormamomentin vaihdellessa. Myös kentänheikennysmenetelmiä kehitetään lähtösuodattimella varustetuille käytöille. Tietokonesimuloinnit ja laboratoriokokeet osoittavat ehdotettujen menetelmien suorituskyvyn laajalla toiminta-alueella nopeuden ja kuormituksen vaihdellessa. Lisäksi tutkitaan lähtösuodattimen vaikutusta modulointimenetelmän valintaan. Jos käytetään yhteismuotosuodatinta, kaksivaihemodulointimenetelmät voivat aiheuttaa liiallista yhteismuotovirran värähtelyä. Tavallinen symmetrinen modulointimenetelmä on sopiva, koska se ei tuota merkittäviä jännitteen yliaaltoja yhteismuotosuodattimen resonanssitaajuuden lähellä. Väitöskirjassa käsitellään myös suodatinsuunnittelua. LC-suodattimen hinta pyritään minimoimaan siten, että suodatusvaatimukset toteutuvat ja liikeanturiton vektorisäätö toimii.

Asiasanat Taajuusmuuttajan lähtösuodatin, oikosulkumoottori, kestomagneettitahtimoottori, anturiton säätö

ISBN (painettu) 978-951-22-9129-8	ISSN (painettu) 1795-2239
ISBN (pdf) 978-951-22-9130-4	ISSN (pdf) 1795-4584
Kieli englanti	Sivumäärä 143

Julkaisija Multiprint Oy

Painetun väitöskirjan jakelu Tehoelektroniikan laboratorio

☒ Luettavissa verkossa osoitteessa http://lib.tkk.fi/Diss/2007/isbn9789512291304/

Preface

The research work for this thesis was carried out in the Power Electronics Laboratory at Helsinki University of Technology. The work was started in October 2003 as a part of a research project dealing with sensorless control of AC motor drives. The project was financed by ABB Oy.

Many people have helped me to complete this thesis. First of all, I would like to thank Prof. Jorma Luomi for his excellent supervision and sincere support. Working with him has taught me about many aspects of academic research and proper English spelling. I would also like to thank Prof. Marko Hinkkanen for his kind guidance and encouragement during this work.

I have greatly enjoyed working with colleagues like Mr. Antti Piippo, Dr. Petri Mäki-Ontto, Mr. Henri Kinnunen, Mrs. Mikaela Ranta, Mr. Konstantin Kostov, and Mr. Toni Tuovinen. Thank you all for creating an inspiring and comfortable research atmosphere. I would also like to thank other members of the laboratory staff: Prof. Jorma Kyyrä, Prof. Seppo Ovaska, Mr. Ilkka Hanhivaara, and Mrs. Anja Meuronen.

I wish also to express my gratitude to people at ABB Oy. The discussions with Mr. Matti Kauhanen, Mr. Mikko Korpinen, Mr. Samuli Heikkilä, Mr. Tuomas Multala, Mr. Matti Mustonen, Mr. Kalle Suomela, Mr. Mikko Vertanen, and Mr. Kari Kovanen helped me to complete this work.

The additional financial support given by the Walter Ahlström Foundation, the Finnish Foundation of Technology, and the KAUTE Foundation is gratefully acknowledged.

Finally, I would like to thank my parents, Pirjo and Hannu Salomäki, for their continuous support throughout my many years of studies. And last, but not least, I would like to express my warmest thanks to my girlfriend, Satu, for her love and support during these years.

Hyvinkää, October 2007

Janne Salomäki

Contents

List of Publications

This thesis consists of an overview and the following publications:

I Salomäki, J. and Luomi, J. (2006). "Vector control of an induction motor fed by a PWM inverter with output LC filter." *European Power Electronics and Drives Association Journal*, **16**(1), pp. 37–43.

II Salomäki, J., Hinkkanen, M., and Luomi, J. (2006). "Sensorless vector control of an induction motor fed by a PWM inverter through an output LC filter." *IEEJ Transactions on Industry Applications*, **126**(4), pp. 430–437.

III Salomäki, J., Hinkkanen, M., and Luomi, J. (2006). "Sensorless control of induction motor drives equipped with inverter output filter." *IEEE Transactions on Industrial Electronics*, **53**(4), pp. 1188–1197.

IV Salomäki, J., Hinkkanen, M., and Luomi, J. (2006). "Influence of inverter output filter on the selection of PWM technique." In *Proc. IEEE-ISIE2006 International Symposium on Industrial Electronics*, pp. 1052–1057, Montreal, Canada.

V Salomäki, J., Piippo A., Hinkkanen, M., and Luomi, J. (2006). "Sensorless vector control of PMSM drives equipped with inverter output filter." In *Proc. 32nd Annual Conference of the IEEE Industrial Electronics Society (IECON'06)*, pp. 1059–1064, Paris, France.

VI Salomäki, J., Hinkkanen, M., and Luomi, J. (2008). "Influence of inverter output filter on maximum torque and speed of PMSM drives." *IEEE Transactions on Industry Applications*, **44**(1). (In press)

VII Piippo A., Salomäki, J., and Luomi, J. (2007). "Signal injection in sensorless PMSM drives equipped with inverter output filter." In *Proc. Fourth Power Conversion Conference (PCC Nagoya 2007)*, pp. 1105–1110, Nagoya, Japan.

VIII Salomäki, J., Hinkkanen, M., and Luomi, J. (2007). "Cost-effective design of inverter output filters for AC drives." In *Proc. 33rd Annual Conference of the IEEE Industrial Electronics Society (IECON'07)*, pp. 1220–1226, Taipei, Taiwan.

The author has written Publications I – VI and VIII with the help and guidance of Prof. Luomi and Prof. Hinkkanen. The author is responsible for the design, analysis, simulations, and experiments. In Publication V, Mr. Piippo helped with the construction of the system model, with the linearization analysis, and with the experimental setup.

Publication VII has been mainly written by Mr. Piippo. The author is responsible for the literature review, the cascade control structure, and partly for the design of the full-order observer. Mr. Piippo combined the full-order observer and the signal injection method, analyzed the frequency response of the system, and performed the simulations and experiments.

Earlier versions of Publications I – III and VI were presented at conferences (Salomäki and Luomi, 2004), (Salomäki et al., 2005b), (Salomäki et al., 2005a), (Salomäki et al., 2007).

Symbols and Abbreviations

Symbols

$\underline{\mathbf{A}}$	System matrix of state-space representation
$\mathbf{A}$	System matrix of state-space representation for PMSM drives
$\mathbf{B}$	System matrix
$\mathbf{C}$	System matrix
C_f	Capacitance of the filter
$\underline{i}_A$	Inverter output current space vector
$\mathbf{i}_A$	Inverter output current vector for PMSM drives
$i_{Ad},\ i_{Aq}$	Real and imaginary components of $\underline{i}_A$ or direct- and quadrature-axis components of $\mathbf{i}_A$
$\underline{i}_R$	Rotor current space vector
$\underline{i}_s$	Stator current space vector
$\mathbf{i}_s$	Stator current vector for PMSM drives
$i_{sd},\ i_{sq}$	Real and imaginary components of $\underline{i}_s$ or direct- and quadrature-axis components of $\mathbf{i}_s$
j	Imaginary unit
$\mathbf{J}$	Rotational matrix
$\underline{\mathbf{K}}$	Observer gain
$\mathbf{K}$	Observer gain for PMSM drives
K_p	Adaptation proportional gain
K_i	Adaptation integral gain
L_d	Direct-axis stator inductance
L_f	Inductance of the filter inductor
L_M	Magnetizing inductance
L_q	Quadrature-axis stator inductance
L'_s	Stator transient inductance
$\mathbf{L}_s$	Stator inductance matrix
p	Number of pole pairs

Q	Quality factor
R_{Lf}	Series resistance of the filter inductor
R_R	Rotor resistance
R_s	Stator resistance
s	Laplace variable
u	Voltage
$u_a,\ u_b,\ u_c$	Phase voltages
$\underline{u}_A$	Inverter output voltage space vector
$\mathbf{u}_A$	Inverter output voltage for PMSM drives
$u'_{A,\mathrm{ref}}$	Magnitude of the unlimited inverter output voltage reference
$u_{Ad},\ u_{Aq}$	Real and imaginary components of $\underline{u}_A$ or direct- and quadrature-axis components of $\mathbf{u}_A$
$\hat{u}_c$	Amplitude of a carrier excitation signal
u_{cm}	Common-mode voltage
u_{dc}	DC-link voltage
$\underline{u}_s$	Stator voltage space vector
$\mathbf{u}_s$	Stator voltage vector for PMSM drives
$u_{sd},\ u_{sq}$	Real and imaginary components of $\underline{u}_s$ or direct- and quadrature-axis components of $\mathbf{u}_s$
t	Time
T_e	Electromagnetic torque
$\underline{\mathbf{x}}$	State vector of state-space representation
$\mathbf{x}$	State vector of state-space representation for PMSM drives
$\underline{x}^s$	Space vector in the stationary reference frame
$x_a,\ x_b,\ x_c$	General phase quantities
$x_\alpha,\ x_\beta$	Real and imaginary parts of $\underline{x}^s$
x_0	Zero-sequence component
γ_f	Gain for the field-weakening control
$\gamma_p,\ \gamma_i$	Proportional and integral gains for the signal injection method
ε	Error signal for the signal injection method
θ_s	Angle of the rotor flux linkage
τ_r	Rotor time constant
τ'_σ	Time constant
ϕ	Angle that changes the direction of the error projection
ψ_{pm}	Permanent magnet flux linkage
$\boldsymbol{\psi}_{pm}$	Permanent magnet flux linkage vector

$\underline{\psi}_R$	Rotor flux linkage space vector
$\underline{\psi}_s$	Stator flux linkage space vector
$\boldsymbol{\psi}_s$	Stator flux linkage vector for PMSM drives
ω_c	Angular frequency of a carrier excitation signal
ω_k	Angular frequency of an arbitrary reference frame
ω_m	Electrical angular speed of the rotor
ω_s	Angular frequency of the rotor flux linkage

Complex-valued variables are underlined and complex conjugates are marked by the symbol *. Vectors and matrices are denoted by bold letters and matrix transposes are marked by the symbol ^{T}. Estimates are marked by the symbol $\hat{}$. Reference values are marked by the subscript ref.

Abbreviations

AC	Alternating current
A/D	Analog-to-digital (converter)
BR	Breaking resistor
CM	Common mode
DC	Direct current
DPWM	Discontinuous pulse-width modulation
du/dt	Rate of change of voltage
DM	Differential mode
DTC	Direct torque control
FW	Field weakening
IGBT	Insulated gate bipolar transistor
IM	Induction motor
IPMSM	Interior permanent magnet synchronous motor
LC	Inductance-capacitance (filter)
LCR	Inductance-capacitance-resistance (filter)
MTPA	Maximum torque-per-ampere
PMSM	Permanent magnet synchronous motor
PWM	Pulse-width modulation
SPWM	Sinusoidal pulse-width modulation
SVPWM	Space vector pulse-width modulation
THD	Total harmonic distortion
VSD	Variable-speed drive

Chapter 1

Introduction

Electric motors consume more than half of all electric energy used in Europe. Most of the motors are alternating current (AC) motors. In particular, three-phase induction motors (IMs) are commonly used in industry, because they are simple in design, reliable, and inexpensive. Permanent magnet synchronous motors (PMSMs) are increasing in popularity due to their high efficiency and power density. In many motor drive applications, precise speed or torque control is needed, which is possible by using a frequency converter between the mains and the motor. Electric energy can also be saved if the motor speed is adjustable. Variable-speed drives (VSDs) are today standard technology in elevators, cranes, conveyors, paper machines, and electrically driven vehicles. Despite the wide use of VSDs in some fields, there is still plenty of potential for energy savings by means of replacing fixed-speed drives with VSDs (de Almeida et al., 2005).

A typical frequency converter consists of a rectifier, a DC link, and an inverter. Voltage-source converters, which have an energy storage capacitor in the DC link, are widely used particularly in commercial VSDs. The output voltage of the inverter is controlled according to pulse-width modulation (PWM). In converter-fed motors, however, problems may appear due to the pulse-width modulated voltage. The sharp-edged voltage pulses produce high voltage stresses in the motor insulations, which may cause winding breakdowns. High voltage peaks are likely to occur, especially in drives with a long motor cable (Persson, 1992). Lower-order harmonics may cause excessive heating and acoustic noise inside the motor. The three-phase inverter inherently produces a common-mode (CM) voltage, which may cause leakage currents to the ground. Bearing currents may also occur, which are a common reason for premature bearing failures (Chen et al., 1995). These harmful phenomena can be avoided, or at least their impact can be reduced, by adding a filter to the output of the inverter. The filtering enhances the efficiency of the motor, mitigates the voltage reflections in the motor cable, and reduces the acoustic noise of the motor. Major disadvantages of adding output filtering are extra cost, added mounting space, and losses in the filter.

Inverter output filters can be divided into du/dt filters and sinusoidal filters. The cut-off frequency of du/dt filters is above the switching frequency of the inverter, and they just reduce the rate of change of the voltage. These filters do not affect the motor control. The cut-off frequency of sinusoidal filters is below the switching frequency, which results in nearly sinusoidal output voltage. A typical topology is a three-phase inductance-capacitance (LC) filter, which mainly filters the differential-mode (DM) voltage. Fig. 1.1 shows an example of phase to phase voltages before and after a sinusoidal filter.

The addition of a sinusoidal output filter to a VSD makes the motor control more dif-

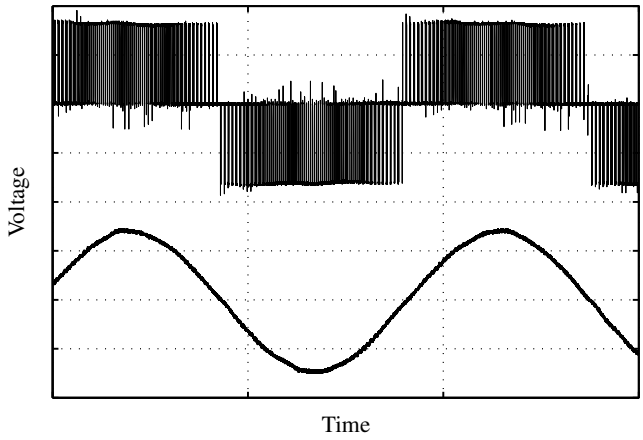

Figure 1.1. Phase to phase voltage before and after sinusoidal filter.

ficult. When an LC filter is used, a simple open-loop method, known as scalar control or constant voltage-per-hertz control, is usually chosen. More sophisticated closed-loop control methods, vector control and direct torque control (DTC), are problematic to implement because of the filter resonance, the difference between inverter and stator currents, and the voltage drop in the filter inductor. When designing vector control, the filter dynamics should be taken into account in addition to the motor dynamics. The vector control needs information about instantaneous values of the stator voltage and the stator current. Therefore, extra measurements may be required because of the filter. Current transducers are typically located at the inverter output. If a filter is connected between the inverter and the motor, the current and voltage measurements from the motor side of the filter require additional sensors, wiring, and analog-to-digital (A/D) converters. In the literature, vector control of VSDs equipped with a sinusoidal filter has not been investigated much. Some control methods that take the inverter output filter into consideration have been proposed (Zimmermann, 1988; Rapp and Haag, 1997; Nabae et al., 1992; Kojima et al., 2004). In these methods, extra current or voltage sensors have to be used because of the filter.

Sensorless control methods have been a hot topic in the field of VSDs during the latest two decades. In this context, the term *sensorless* means that no speed or position sensor is used. Advantages of sensorless drives are reduced hardware complexity, lower cost, increased reliability, and less maintenance requirements (Holtz, 2002). There is a vast variety of different sensorless control methods for both IM and PMSM drives (Hinkkanen, 2004b; Eskola, 2006). Among the most promising methods are adaptive full-order observers developed by Kubota et al. (1993) and Yang and Chin (1993) for IM drives and by Yang et al. (1993) for PMSM drives. If it were possible to control AC drives equipped with an inverter output filter with sensorless methods, the above-mentioned advantages would also apply to these drives.

A three-phase voltage-source inverter produces phase voltages with an instantaneous sum that is not zero, i.e. a CM voltage is generated. The CM voltage at the inverter output can be reduced by means of a CM filter. The CM filter is usually built so that the star point of the capacitors of the differential-mode LC filter is connected to the DC link. In addition, the CM filter typically includes a CM inductor and a damping resistor. CM filtering does not affect the vector control of the motor because the control is based on DM quantities.

However, the CM filter may cause a high CM current if the CM inductor saturates (Akagi et al., 2004). Akagi investigated CM filtering using only one PWM method. The saturation of the CM inductor is likely to occur if the CM filter resonance is excited by the PWM. The influence of different PWM techniques on the CM filtering has not yet been investigated.

The cost of an inverter output filter is not negligible as compared to the total cost of the AC drive (Finlayson, 1998). Thus, the cost-effective design of the filter is important. The filtering performance can be improved if the resonance frequency of an LC filter is decreased. However, the cost of the filter is approximately inversely proportional to the resonance frequency. The filtering requirements are usually determined by the total harmonic distortion (THD) of the stator voltage, the THD of the inverter output current, and the voltage drop in the filter inductor. Vector control may also set requirements for the filter design. In the literature, the filter design has not been considered from the control point of view.

The main aim of the thesis is to develop sensorless vector control methods for IM and PMSM drives that are equipped with an LC filter at the inverter output. The control methods should meet the following requirements:

- No extra measurements should be applied due to the filter, thus enabling the use of the filter in a standard frequency converter without any hardware modifications.
- The performance of the developed control methods should be close to that of drives without the filter.
- The control methods should include field weakening for high speed operation.

Additional objectives of the thesis are:

- to find a suitable topology for CM filtering and investigate possible problems caused by the CM filter.
- to minimize the filter cost so that the filtering requirements are fulfilled and the vector control is workable.

The thesis consists of this overview and eight publications. In Chapter 2, a description of the system is presented and problems caused by the PWM are discussed. Then a short review of inverter output filters is presented. The chapter concludes with design aspects of sinusoidal filters.

In Chapter 3, the control of IM drives equipped with an LC filter is considered. The system model is presented, after which state-of-the-art control methods are reviewed. The chapter continues with presenting a cascade control structure and a full-order observer. The observer is augmented with a speed-adaptation mechanism resulting in the proposed speed-sensorless control method. Finally, an experimental comparison of the control performance with and without an LC filter is shown.

Chapter 4 deals with the control of permanent magnet synchronous motor drives equipped with an LC filter. The system model is introduced, after which state-of-the-art control methods are reviewed. A cascade control structure similar to one used for the IM drive is presented. The proposed speed-adaptive full-order observer is introduced and, finally, the addition of a signal-injection method is discussed.

Chapter 5 describes the experimental setup used in this work. Technical data and descriptions of the hardware and software are given. Chapter 6 summarizes the publications and describes the scientific contribution of the thesis. Chapter 7 concludes the thesis.

Chapter 2

Voltage-Source Converter and Output Filters

In this chapter, a three-phase voltage-source converter and output filters are introduced. After showing the converter topology, the most important PWM methods are reviewed and the problems caused by the PWM are dealt with. The influence of an inverter output filter on the required measurements in an AC drive is discussed. Then, a review of passive inverter output filters is presented. Different filter topologies are shown, after which the design aspects of differential-mode (DM) and common-mode (CM) LC filters are discussed.

2.1 Voltage-Source Converter

Fig. 2.1 shows a circuit diagram of a three-phase voltage-source converter (Mohan et al., 1995). A diode bridge rectifies the AC mains voltage to a DC voltage. A DC-link capacitor provides an energy storage for reducing the ripple in the rectified voltage. A two-level inverter converts the DC voltage to an adjustable AC voltage for the motor. The inverter consists of power electronic switches, which are usually insulated gate bipolar transistors (IGBTs). An output filter is useful if the adverse effects of the inverter must be attenuated. Alternatives to the voltage-source converter are current-source converters and matrix converters.

Each output phase of the inverter can be switched either to the positive or negative

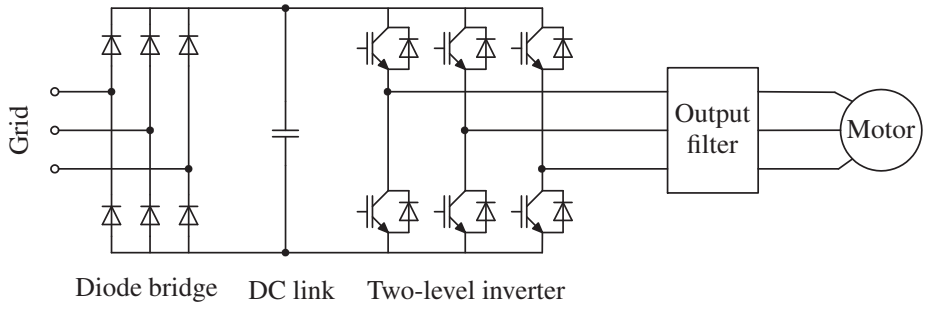

Figure 2.1. Circuit diagram of voltage-source converter equipped with inverter output filter.

bus of the DC link. There are a total of eight possible combinations of switching states. Switching states correspond to six active space vectors and two zero space vectors for the inverter output voltage. A desired output voltage is obtained by combining the switching states using PWM. A wide variety of different modulation techniques have been proposed. The most used ones are reviewed in the following.

Pulse-Width Modulation Techniques

Schönung and Stemmler (1964) presented the classical sinusoidal pulse-width modulation (SPWM) method, in which a triangular carrier signal is compared with a sinusoidal reference signal in each phase. This method is the basis for state-of-the-art PWM techniques. A disadvantage of the SPWM method is the limited linear output voltage range.

The addition of a zero-sequence component to the voltage references was an important improvement, because the linear voltage range can be increased. The modulation method developed by King (1974) has later been implemented more effectively and called the symmetrical suboscillation method by Svensson (1988) or space vector PWM (SVPWM) by van der Broeck et al. (1988). The method produces equal on-times for both zero vectors during a switching period. The SVPWM maximizes the linear output voltage range. The method based on the injection of a third harmonic (Houldsworth and Grant, 1984) has also gained popularity, but its linear voltage range is not as high as that of the SVPWM method.

Two-phase modulation methods, also known as discontinuous PWM (DPWM) (Depenbrock, 1977; Ogasawara et al., 1989; Kolar et al., 1991; Hava, 1998), have been developed to reduce the switching losses in the inverter. The switching losses are reduced, because one phase is kept unswitched during a switching period. These methods usually have the same linear voltage range as the SVPWM method. The DPWM methods cause high lower-order harmonics in the CM voltage.

Pulse-width modulation techniques that reduce the CM voltage have also been proposed (Cacciato et al., 1999; Lai, 1999; Lai and Shyu, 2004). These methods are usually based on the replacement of the zero vectors by active vectors, which causes an increased current ripple.

Problems Caused by PWM Voltage

Modern voltage-source inverters with IGBT switches generate steep voltage pulses. The rate of change of the voltage (du/dt) is typically between 1 kV/µs and 5 kV/µs. The high du/dt enables lower switching losses, and thus a higher switching frequency can be used. However, sudden alterations of the inverter output voltage can cause high-frequency oscillations and voltage overshoots (Persson, 1992; von Jouanne et al., 1995). The high du/dt of the inverter output voltage can be hazardous, especially, if a long motor cable is used between the inverter and the motor. The amplitude of the voltage overshoot at motor terminals may be nearly two times the DC-link voltage. In particular, windings of old motors that are not designed for a converter supply can be damaged due to the high voltage stresses.

The common-mode voltage (i.e. zero-sequence component of the voltage) is defined as

$$u_{cm} = \frac{1}{3}\left(u_a + u_b + u_c\right) \tag{2.1}$$

The sum of the phase to neutral voltages u_a, u_b, and u_c at the inverter output is always

different from zero. Thus, the three-phase inverter inherently produces a CM voltage. The CM voltage and CM currents through parasitic capacitances in the motor are major causes of bearing currents. Capacitive bearing currents are generated due to the high du/dt of the inverter output voltage. These harmless bearing currents flow through the parasitic capacitances of the bearings. More severe discharge mode bearing currents occur when the voltage across the inner and outer race of the bearing exceeds its threshold value and results in a discharge through the lubricant film (Chen et al., 1995). The discharge mode bearing currents are a concern especially in small motors (Muetze and Binder, 2005). Circulating bearing currents have been reported by Chen et al. (1996) and in more detail explained by Mäki-Ontto (2006). They are caused by a shaft voltage which is induced by a magnetic flux encircling the shaft. The magnetic flux is excited by the high-frequency CM current. Circulating bearing currents cause problems mainly in big motors, typically above 100 kW (Muetze and Binder, 2005). Ollila et al. (1997) have presented a bearing current type which may occur if the rotor is connected to the ground with a significantly lower impedance path than the stator housing.

The additional losses due to the PWM may cause overheating inside the motor. The iron losses can be even 50% higher in the inverter-supplied motor than in the grid-supplied motor (Green et al., 2003). The audible noise level of the motor is clearly increased due to the inverter supply. As stated by Belmans et al. (1987), high noise levels may be expected when the inverter output voltage contains harmonics at the natural frequency of the stator. In order to mitigate the harmful effects of the PWM, filters can be used at the inverter output. Different passive filter topologies are reviewed in Sections 2.2 and 2.3.

Measurements in AC Drives

Feedback from the system is needed in order to have precise control over the torque and speed of the motor. Fig. 2.2 shows an AC drive in which an output filter is connected between the inverter and the motor. The drive is equipped with measurements from the DC-link voltage u_{dc}, the inverter output current $\underline{i}_A$, inverter output voltage $\underline{u}_A$, the stator current $\underline{i}_s$, the stator voltage $\underline{u}_s$, and the rotor speed ω_m. This amount of measurements would require many sensors, A/D converters, and signal wires to be connected to the frequency converter. A reduction in the number of measurements is highly desirable.

A standard frequency converter, which is designed to be used without an inverter output filter, contains only the inverter output current measurement and possibly the DC-link

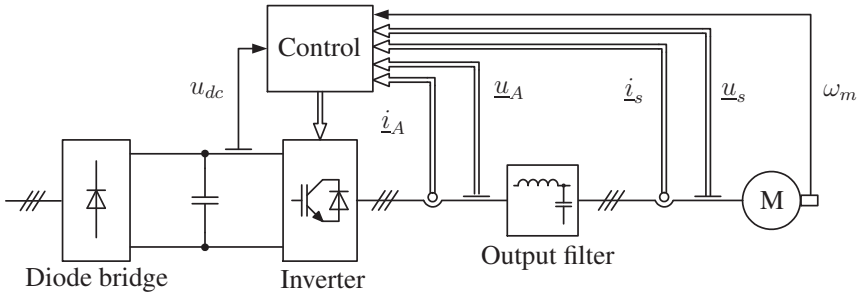

Figure 2.2. Possible measurements in AC drive when inverter output filter is used. Double lines indicate complex quantities (space vectors) whereas single lines indicate real quantities (scalars)

voltage and the rotor speed measurements. Typically, the vector control of AC motors needs feedback from the stator current, the stator voltage, and the rotor speed (or position). If an output filter is not used, the inverter output current equals the stator current (with the exception of high-frequency phenomena due to parasitic capacitances of the motor cable). The feedback for the stator current control is provided by current sensors at the inverter output. On the other hand, if an output filter is used, the inverter output current differs from the stator current. Therefore, current sensors at the inverter output do not directly provide a feedback for the stator current control. Adding current sensors to the motor side of the filter is one possible solution, but it would require additional hardware (wiring, A/D converters, etc.) to a standard frequency converter.

If an inverter output filter is not used, the direct measurement of the stator voltage is problematic because of the PWM output voltage. Filtering of the measured stator voltage causes a harmful delay in the control. Typically, the stator voltage is calculated from the DC-link voltage and the inverter switching states. The DC-link voltage is ideally constant, but in practice it depends on the mains voltage and load conditions. The DC voltage ripple may cause torque and speed variations in the motor. The ripple is usually compensated by measuring the DC-link voltage (Pedersen et al., 1993). The calculated stator voltage may also be inaccurate because of the inverter nonidealities. Inverter nonidealities include dead-time effect (Murai et al., 1987), minimum pulse width limitation, changes in the slope of the rising and falling edges of the inverter output voltage due to parasitic capacitances of the semiconductors (Sepe and Lang, 1994), zero-current clamping during the dead time (Murai et al., 1992b; Choi and Sul, 1995), and voltage drops in the semiconductors. In this thesis, simple current feedforward compensation for dead times and semiconductor voltage drops was used in a fashion similar to Pedersen et al. (1993).

If a sinusoidal filter is used at the inverter output, the stator voltage does not contain a significant amount of harmonics, and the direct measurement of the stator voltage is possible. Nevertheless, the stator voltage measurement would require additional hardware to a standard frequency converter.

Information about the rotor speed is necessary for the speed control and it is useful in estimating the magnetic flux for the vector control. In synchronous motor drives, rotor position information is essential for the vector control. The rotor speed or position can be measured using a motion sensor that is mounted on the motor shaft. Alternatively, the rotor speed or position can be estimated using sensorless control techniques.

If an inverter output filter is used, the ideal solution for the vector control would be a method that does not need any additional measurement. If the vector control is possible measuring only the inverter output current and the DC-link voltage, an output filter can be added to a standard frequency converter without any hardware modifications.

2.2 Output Inductors

A simple and low-cost method for low-pass filtering of the inverter output voltage is to use output inductors as shown in Fig. 2.3. Output inductors are also known as output chokes, motor chokes, or series reactors. The topology provides an additional inductance to the system, which results in a lower du/dt at the motor terminals. Output inductors are mainly used to reduce motor insulation stress. They have limited effect on the induced shaft voltage and EMI (von Jouanne et al., 1998). According to Hanigovszki et al. (2003), output inductors increase the CM oscillations when a long cable is used. Output inductors

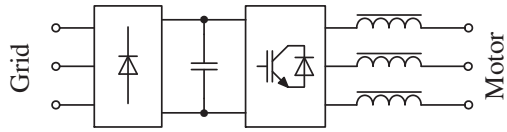

Figure 2.3. Output inductors.

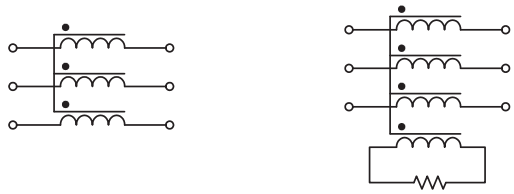

(a) (b)

Figure 2.4. (a) Common-mode inductor, (b) common-mode transformer.

are usually built on a three-legged laminated steel core, but also three separate cores can be used. Acoustic noise due to the magnetostriction can be reduced by using iron powder pot cores (Hanigovszki et al., 2003).

A means to reduce the CM current is to add a CM inductor to the inverter output as illustrated in Fig. 2.4(a). Either wound or feed-through toroidal CM chokes can be used (Muetze, 2005). Since the CM inductor should maintain its inductive characteristics up to a few MHz, the core material is usually ferrite. Low-loss ferrite cores may cause extended ringing due to a low damping factor (Finlayson, 1998). Thus, additional damping is usually needed. Fig. 2.4(b) shows one solution developed by Ogasawara and Akagi (1996). A damping resistor is connected to the terminals of an additional winding. According to Ogasawara and Akagi, the size of this CM transformer is one third of the conventional CM inductor.

2.3 LC Filters

Output inductors are not always sufficient to mitigate high frequencies from the inverter output voltage. LC filters are more effective than output inductors. A basic LC filter topology is shown in Fig. 2.5(a). It consists of three inductors and three capacitors. Many modifications of this topology have been presented. Depending on the cut-off frequency, the filters can be divided into du/dt filters and sinusoidal filters. The cut-off frequency of the du/dt filter is above the switching frequency of the inverter, whereas the cut-off frequency of the sinusoidal filter is below the switching frequency. Fig. 2.6 shows an example of the magnitude response from the inverter output voltage to the stator voltage, when an LC filter is connected to an IM drive. The cut-off frequency of the system, i.e. the frequency where the magnitude response is -3 dB, is approximately 1.8 kHz. If the switching frequency is, for example, 5 kHz, the filter attenuates the switching noise effectively.

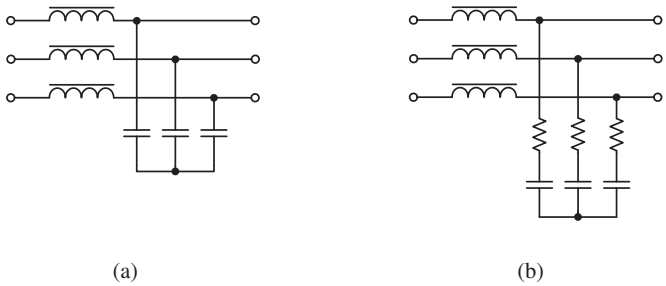

Figure 2.5. (a) Three-phase LC filter, (b) three-phase LCR filter.

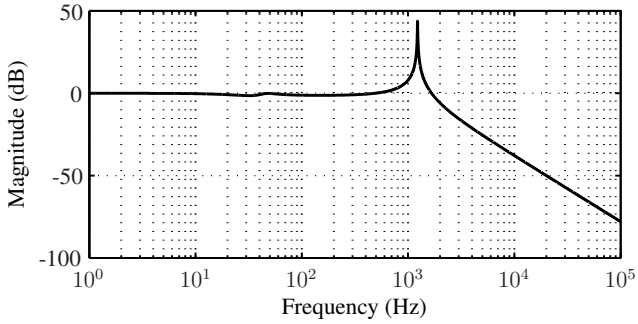

Figure 2.6. Magnitude response from inverter output voltage to stator voltage in IM drive equipped with LC filter.

du/dt Filters

An LCR filter, shown in Fig. 2.5(b), has been used to decrease the differential-mode du/dt of the inverter output voltage (von Jouanne and Enjeti, 1997). Filter resistors are used to obtain an overdamped circuit and to absorb the reflected energy. The filter effectively reduces motor terminal overvoltages. Another du/dt filter topology, proposed by Rendusara and Enjeti (1998), is shown in Fig. 2.7. The star point of the LCR filter capacitors is connected to the DC-link midpoint. This topology reduces both DM and CM du/dt. Significant reductions in motor terminal overvoltages, high-frequency leakage currents, and induced shaft voltages can be obtained. If the DC-link midpoint is not available, the filter topology presented by Palma and Enjeti (2002) can be used. Two neutral points obtained by using six resistors and six capacitors are connected to the positive and negative DC buses, respectively.

Kim and Sul (1997d) proposed a clamping filter shown in Fig. 2.8. Six clamping diodes are used to connect each phase to both positive and negative DC buses. The topology decreases the du/dt at the motor terminals and, in addition, removes the voltage peaks due to ringing. The advantages of this topology compared to the LCR filter are smaller size and smaller power losses. In another clamping filter, presented by Hanigovszki et al. (2004), the star point of the filter capacitors is connected to the DC link using only two diodes as shown in Fig. 2.9. This topology also reduces motor terminal voltage overshoot significantly.

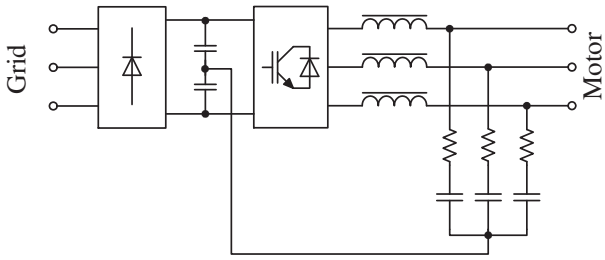

Figure 2.7. LCR filter with connection to DC-link midpoint (Rendusara and Enjeti, 1998).

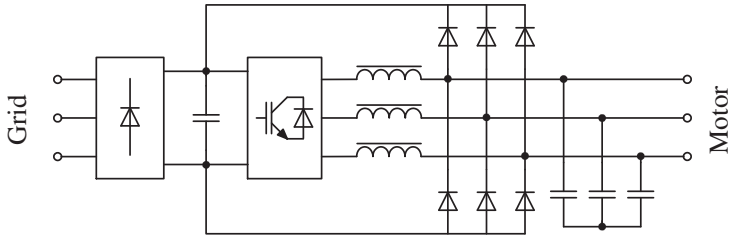

Figure 2.8. Clamping filter with six diodes (Kim and Sul, 1997d).

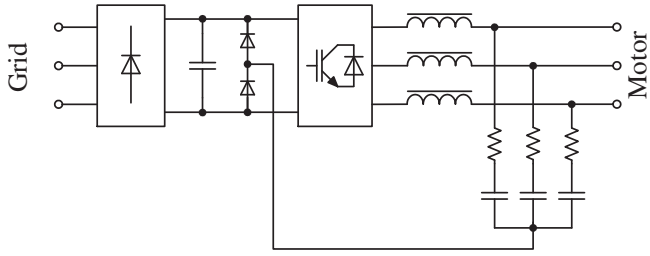

Figure 2.9. Clamping filter with two diodes (Hanigovszki et al., 2004).

Sinusoidal Filters

An LC filter, shown in Fig. 2.5(a), is the basic filtering device when close to a sinusoidal voltage waveform is needed. The sinusoidal LC filter does not require an additional resistor if the inverter output voltage does not include significant harmonics near the system resonance frequency. Usually, the internal resistance of the inductor is sufficient. A weakness of this topology is that it does not filter the CM voltage. Various sinusoidal filters reducing both DM and CM voltages have been proposed. Murai et al. (1992a) connected the star point of the LC filter capacitors to the negative DC bus in order to provide a route for a CM current (Fig. 2.10). The six diodes are only optional; they are not needed if the switching frequency is high. The filter substantially suppresses the leakage currents of the motor.

The topology shown in Fig. 2.11 was proposed by Akagi et al. (2004). A separate CM inductor is added in front of an LCR filter, and the star point of the filter capacitors is connected to the negative DC bus through a series connected capacitor and resistor. An advantage of this topology is that the DM and CM filters can be designed separately.

Fig. 2.12 shows an "all-cure filter" introduced by Hanigovszki (2005). The filter consists of separate DM and CM filters with DC link connections to both negative and positive DC buses. The left-hand side CM inductor is meant to filter the frequencies in the range of the switching frequency. The right-hand side CM inductor is added in order to filter frequencies above 150 kHz. According to Hanigovszki, the filter reduces motor insulation and bearing stress, acoustic switching noise, and high-frequency emissions to the mains. Furthermore, when using the filter, the motor cable length does not need to be limited.

Several output filter topologies that are based on the CM transformer have been presented (Murai et al., 1992a; Swamy et al., 2001; Chen et al., 2007). Fig. 2.13 shows the topology of a "potential-type suppression circuit" proposed by Murai et al. (1992a). The Y-connected resistors and capacitors provide an artificial neutral point, which is connected to the ground through an additional winding of the CM transformer. The CM voltage at the artificial neutral point generates a CM current through an additional winding of the CM transformer. The CM current induces a voltage, equal to the CM voltage, across the other windings of the CM transformer and cancels the CM voltage at the motor terminals. The output filter in Fig. 2.14 is a combination of a differential-mode LCR filter and a CM transformer with one winding connected to the DC-link midpoint (Chen et al., 2007). As compared to the topology in Fig. 2.11, the filter by Chen et al. needs one capacitor less, but it requires one winding more in the CM transformer. The analysis of the CM circuit is more complicated for the filter by Chen et al. than for the filter by Akagi et al. (2004).

Selection of Filter

A three-phase LC filter shown in Fig. 2.5(a) was selected in this thesis, because it is a widely used topology for DM sinusoidal filters. An LC filter was used in Publications I–III and V–VIII. A slightly modified version of the topology shown in Fig. 2.11 was selected in Publication IV to investigate the suitability of different PWM methods. The modification was that the three-phase LCR filter was replaced by a three-phase LC filter. The topology was selected because it filters both DM and CM voltages effectively, and the CM circuit is simple to analyze. It also has well-documented design rules by Akagi et al. (2004).

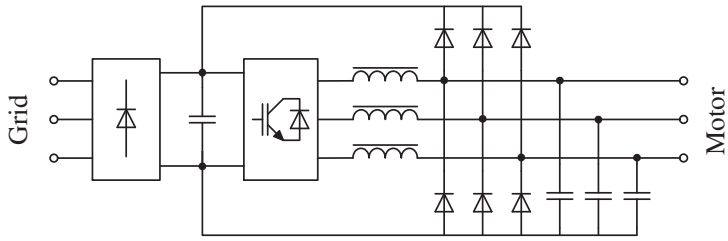

Figure 2.10. Sinusoidal filter with clamp circuit and connection to negative DC bus (Murai et al., 1992a).

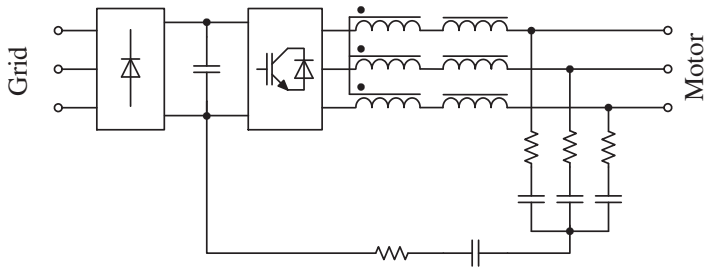

Figure 2.11. Sinusoidal filter with connection to negative DC bus (Akagi et al., 2004).

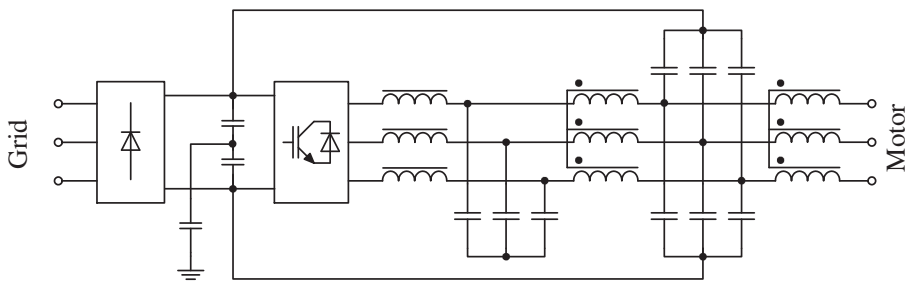

Figure 2.12. "All-cure filter" (Hanigovszki, 2005).

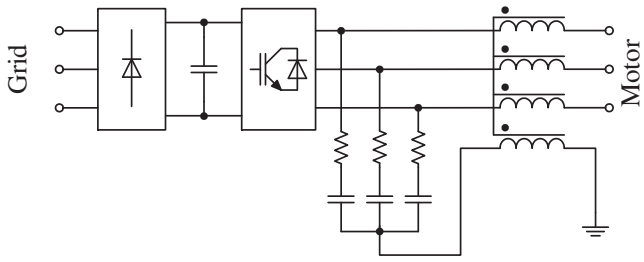

Figure 2.13. CM filter with artificial neutral point connected to ground through CM transformer (Murai et al., 1992a).

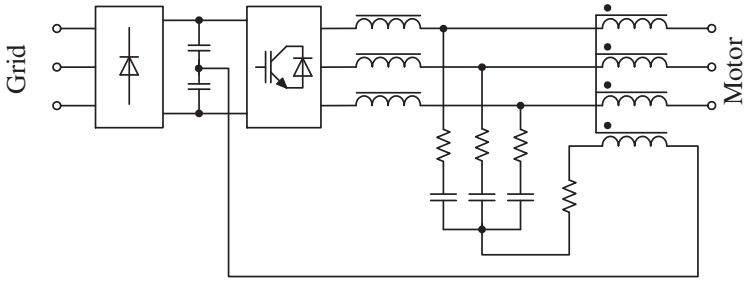

Figure 2.14. Differential and CM filter with CM transformer (Chen et al., 2007).

2.4 Design Aspects of Sinusoidal Filters

The inverter output filter can be designed basing on different design criteria. These criteria may include filtering performance, filter size and cost, losses in the filter, losses in the whole drive, influence on the load capability, and influence on the control. Usually, the design is a compromise between the filtering performance and the cost. In this section, the design aspects of both DM and CM sinusoidal output filters are reviewed.

Differential-Mode Filter Design

Sinusoidal filters are usually second-order low-pass filters, meaning that the topology is either LC or LCR. The selection of the resonance frequency[1] is important, because it determines the width of the pass band. In the stop band, the voltage attenuation slope is 40 dB/decade as shown in Fig. 2.6. van der Broeck and Loef (1995) chose the resonance frequency to be one tenth of the switching frequency in order to have the total distortion factor[2] of the stator voltage less than 1%. Xiyou et al. (2002) proposed a design method where the THD of the motor voltage is preferably less than 5%, resulting in the resonance frequency that is 30% of the switching frequency. Hanigovszki (2005) introduced a condition for the cut-off frequency of the filter: the cut-off frequency should be at least ten times higher than the highest fundamental frequency and less than half of the switching frequency.

[1]The resonance frequency is defined as $f_{\mathrm{res}} = \frac{1}{2\pi\sqrt{LC}}$.

[2]The RMS of the harmonics divided by the RMS of the signal

Another design criterion is the voltage drop in the filter inductor at the nominal operating point of the motor. If the fundamental frequency is high, the voltage drop may rise to unacceptable values. Xiyou et al. (2002) required the voltage drop to be less than 5% of the rated output voltage at the nominal speed.

The filter capacitors provide a low-impedance route for high-frequency currents. These currents are limited mainly by the filter inductor. In some filter design papers, a limit is specified for the harmonic content of the inverter output current. Xiyou et al. (2002) limited the harmonic content to be less than 20% of the rated current capacity of the drive. Akagi et al. (2004) set the limit to 10%.

The cost of the inverter output filter may be significant, and thus the component prices should be taken into account in the filter design. Seguier and Labrique (1993) simply used the product of the inductance and the capacitance to estimate the filter price. A more sophisticated approximation was used by Wheeler and Grant (1997) and Xiyou et al. (2002). The cost of the inductor and capacitor was approximated by a linear function of the power rating of the component. In addition to the component prices, the cost of the filter is composed of the enclosure cost, the manufacturing cost, and the possible cooling cost. These costs are difficult to be included in the filter design and, therefore, they are not taken into account.

In Publication VIII, the THD of the stator voltage is limited to 4%, the THD of the inverter output current is limited to 20%, and the voltage drop in the filter inductor is limited to 3% in the nominal operating point. The resonance frequency of the system is suggested to be less than 25% of the sampling frequency in order to have workable vector control. Filter component costs are taken into account in a fashion similar to Xiyou et al. (2002). Furthermore, the inverter cost is taken into account in order to find an optimum switching frequency that minimizes the total cost of the filter and the inverter power stage. According to the results in Publication VIII, the filter designed according to the proposed design procedure fulfils the filtering requirements and the vector control works properly.

Common-Mode Filter Design

The CM filter design is affected by the DM filter, because DM filter components are a part of the CM circuit. For example, the filter in Fig. 2.11 has all DM filter components in the CM circuit. Therefore, the CM filter should be designed after the DM filter.

The CM inductor design is an important part of the CM filter design. The inductor should be designed so that the core does not saturate, because the saturation may lead to excessive CM currents. Akagi et al. (2004) have designed the CM inductor such that the maximum flux density inside the CM inductor core, at the fundamental frequency of 40 Hz, is half of the saturation flux density of the core material. Akagi et al. have shown that the CM inductor core does not saturate in the worst operation point, i.e. in the operation point where the reference of the inverter output voltage is zero. A more straightforward way to design the CM inductor would be to limit the maximum flux density below the saturation flux density directly in the worst operation point. Hanigovszki (2005) has limited the CM current to be less than 25% of the nominal current of the drive. Due to this limitation, a high CM inductance is needed in low-power drives (less than 0.75 kW) at a typical switching frequency of 5 kHz.

After the CM inductance is determined, the capacitance of the CM filter is selected so that the desired resonance frequency of the CM filter is obtained. Akagi et al. (2004) have set the resonance frequency to $1/10 \ldots 1/6$ times the switching frequency. The resistor of

the CM filter is selected so that the quality factor[3] of the filter is between 5 and 8.

Chen et al. (2007) have presented a design method for a CM filter based on the CM transformer. All self and mutual inductances of the CM transformer are set equal at a value that is 2 . . . 3 times the inductance of the DM filter. The resistor of the CM filter is selected so that the quality factor is between 1 and 5.

Common-mode filtering may cause problems when certain PWM methods are used. According to Publication IV, two-phase modulation methods (also known as discontinuous PWM methods) are not suitable when a sinusoidal CM filter is used. The avoidance of the two-phase PWM schemes has already been advised by van der Broeck and Loef (1995), but no analysis or results were presented. Two-phase modulation methods generate significant zero-sequence components close to the resonance frequency of the CM filter. The excitation of the filter resonance causes a high CM current, which saturates the CM inductor. Three-phase modulation methods, e.g. SPWM and SVPWM, do not generate notable zero-sequence components close to the resonance frequency of the CM filter, therefore they are recommended to be used with a sinusoidal CM filter. The starting of the modulation may also cause problems, but they can be solved by modifying the on-durations of the zero vectors as proposed in Publication IV.

[3]The quality factor is defined as $Q = \frac{1}{R}\sqrt{\frac{L}{C}}$

Chapter 3

Control of IM Drives Equipped With an LC Filter

In this chapter, a system model is presented for a three-phase LC filter and an induction motor (IM). State-of-the-art control methods are reviewed for such a system. Then, the cascade control structure, full-order observer, and the speed adaptation mechanism proposed in this thesis are presented. Finally, an experimental comparison of the control performance with and without an LC filter is shown.

3.1 System Model

Space Vectors

Space vectors are useful in the modeling of three-phase systems. They were originally developed by Kovács and Rácz (1959). The space vector represents a three-phase quantity such as current or voltage as a complex quantity $\underline{x}^s$ defined by

$$\underline{x}^s = \frac{2}{3}\left(x_a + x_b e^{j2\pi/3} + x_c e^{j4\pi/3}\right) \tag{3.1}$$

where x_a, x_b, and x_c are the phase quantities that may vary in time. The superscript s indicates that the space vector is expressed in the stationary reference frame. The space vector can be divided into real and imaginary parts: $\underline{x}^s = x_\alpha + jx_\beta$.

The space vectors can be expressed in different reference frames. Coordinate transformation between a general reference frame and the stationary reference frame is

$$\underline{x}^k = \underline{x}^s e^{-j\theta_k} \tag{3.2}$$

where θ_k is the angle of the general reference frame with respect to the stationary reference frame. The space vector expressed in the general reference frame can be divided into real and imaginary parts as $\underline{x}^k = x_d + jx_q$.

The zero-sequence component of the phase quantities is not included in space vectors. If zero-sequence components are needed, they can be treated separately. The definition of the zero-sequence component is

$$x_0 = \frac{1}{3}\left(x_a + x_b + x_c\right) \tag{3.3}$$

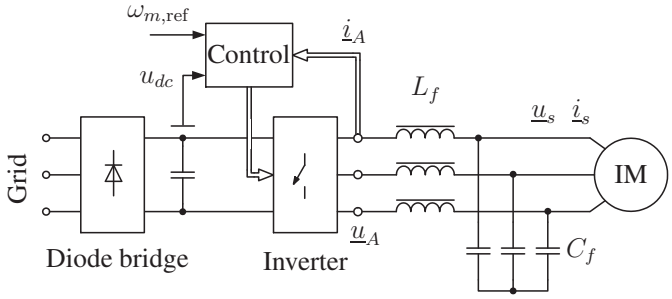

Figure 3.1. Induction motor (IM) drive equipped with three-phase LC filter.

LC Filter and Induction Motor

Fig. 3.1 shows a drive system consisting of a frequency converter, LC filter, and induction motor. The inverter output voltage $\underline{u}_A$ is filtered by an LC filter, and the induction motor is fed by the filtered voltage $\underline{u}_s$. The inverter output current and the stator current are denoted by $\underline{i}_A$ and $\underline{i}_s$, respectively. In a reference frame rotating at angular frequency ω_k, the equations of the LC filter are

$$\frac{d\underline{i}_A}{dt} = -\frac{R_{Lf}}{L_f}\underline{i}_A - j\omega_k\underline{i}_A + \frac{1}{L_f}(\underline{u}_A - \underline{u}_s) \tag{3.4}$$

$$\frac{d\underline{u}_s}{dt} = -j\omega_k\underline{u}_s + \frac{1}{C_f}(\underline{i}_A - \underline{i}_s), \tag{3.5}$$

where L_f is the inductance and R_{Lf} the series resistance of the inductor, and C_f is the capacitance of the filter.

The inverse-Γ model of the induction motor (Slemon, 1989) is used, because it is well suited for control purposes. The model contains only two inductances instead of the three inductances of the conventional T model. The leakage inductance is located at the stator side. The stator and rotor voltage equations are

$$\underline{u}_s = R_s\underline{i}_s + \frac{d\underline{\psi}_s}{dt} + j\omega_k\underline{\psi}_s \tag{3.6}$$

$$0 = R_R\underline{i}_R + \frac{d\underline{\psi}_R}{dt} + j(\omega_k - \omega_m)\underline{\psi}_R, \tag{3.7}$$

respectively, where R_s and R_R are the stator and rotor resistances, respectively, $\underline{i}_R$ is the rotor current, and ω_m is the electrical angular speed of the rotor. The stator and rotor flux linkages are

$$\underline{\psi}_s = (L'_s + L_M)\underline{i}_s + L_M\underline{i}_R \tag{3.8}$$

$$\underline{\psi}_R = L_M(\underline{i}_s + \underline{i}_R), \tag{3.9}$$

respectively, where L'_s denotes the stator transient inductance and L_M is the magnetizing inductance. Fig. 3.2 shows a space vector equivalent circuit for an LC filter and induction motor in the stationary reference frame.

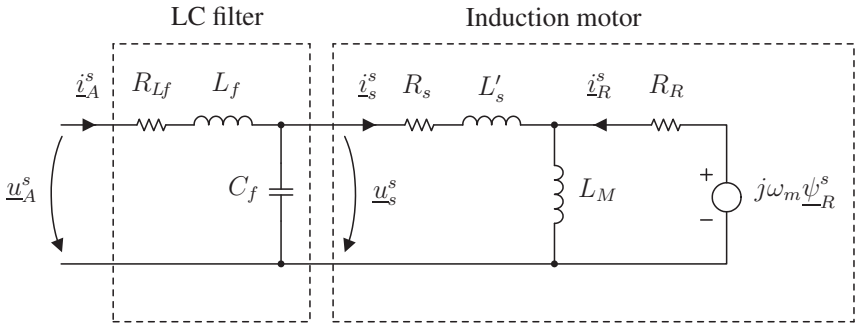

Figure 3.2. Space vector equivalent circuit for LC filter and induction motor in stationary reference frame ($\omega_k = 0$).

State-Space Representation

Based on Eqs. (3.4)–(3.9), a state-space representation of the system can be written as

$$\frac{d\underline{\mathbf{x}}}{dt} = \underbrace{\begin{bmatrix} -\frac{R_{Lf}}{L_f} - j\omega_k & -\frac{1}{L_f} & 0 & 0 \\ \frac{1}{C_f} & -j\omega_k & -\frac{1}{C_f} & 0 \\ 0 & \frac{1}{L'_s} & -\frac{1}{\tau'_\sigma} - j\omega_k & \frac{1}{L'_s}\left(\frac{1}{\tau_r} - j\omega_m\right) \\ 0 & 0 & R_R & -\frac{1}{\tau_r} - j(\omega_k - \omega_m) \end{bmatrix}}_{\underline{\mathbf{A}}} \underline{\mathbf{x}} + \underbrace{\begin{bmatrix} \frac{1}{L_f} \\ 0 \\ 0 \\ 0 \end{bmatrix}}_{\mathbf{B}} \underline{u}_A \tag{3.10}$$

$$\underline{i}_A = \underbrace{\begin{bmatrix} 1 & 0 & 0 & 0 \end{bmatrix}}_{\mathbf{C}} \underline{\mathbf{x}} \tag{3.11}$$

The state vector is $\underline{\mathbf{x}} = \begin{bmatrix} \underline{i}_A & \underline{u}_s & \underline{i}_s & \underline{\psi}_R \end{bmatrix}^T$, and the two time constants are defined as $\tau'_\sigma = L'_s/(R_s + R_R)$ and $\tau_r = L_M/R_R$. The inverter output current is selected as a state variable because it is measured. The stator current is selected as a state variable because its d and q axis components in the rotor-flux-oriented reference frame are proportional to the rotor flux linkage and electromagnetic torque, respectively. The inverter output voltage is the input of the system.

3.2 Control Structures

In the literature, the vector control methods of AC drives equipped with a sinusoidal LC filter are mostly based on cascaded controllers. Zimmermann (1988) has supplemented a field-oriented stator current control with a P control for the stator voltage and a bang-bang control for the filter capacitor current. These two innermost controllers are implemented in the stationary reference frame. The measured feedback signals are the stator current, the stator voltage, the capacitor current, and the rotor speed.

A similar bang-bang control of the capacitor current has been used by Rapp and Haag (1997) for a high-speed IM with an LC filter. The stator current is controlled using a state

controller enhanced with an integral action. The measured feedback signals are the stator current, the stator voltage, the capacitor current, and the rotor speed.

A speed-sensorless control method for an IM drive with an LC filter has been proposed by Petkovšek et al. (2000). The innermost control loop is a bang-bang control for the filter capacitor current. In the next control loop, the stator voltage is regulated by means of a PI controller with a cross-coupling compensation. The rotor speed estimate is based on the motor model and on the feedback from the stator voltage and current.

Nabae et al. (1992) have compensated for the oscillation due to the LC filter using a voltage feedback circuit. The reference of the inverter output current is modified on the grounds of a high-pass filtered stator voltage in the stationary coordinate system. The resulting field-oriented vector control requires measurements of the inverter output current, the stator voltage, and the rotor speed. The method has been later improved by implementing the high-pass filter in a rotating reference frame (Nabae et al., 1994). The results presented in the publication have been obtained without any load connected to the filter output. Jalili et al. (2005) have used a similar high-pass filtered stator voltage feedback for a high-speed IM with an LC filter. The feedback is applied to modify the inverter output voltage reference. The basic problem with these methods is that they ignore the fundamental-wave component of the capacitor current. This simplification causes incorrect field orientation especially at high speeds.

Kojima et al. (2004) have used a field-oriented vector control augmented with a deadbeat controller for the inverter output current and the stator voltage. The advantage of the deadbeat control is the fast response of the LC filter output voltage. The control parameters vary with the fundamental frequency, and they are stored in the memory of a digital signal processor (DSP). The method needs measurements of the inverter output current, the stator voltage, the stator current, and the rotor speed.

The control method proposed in Publication I consists of cascaded controllers and a full-order observer. The system states are estimated using the observer, and no additional stator current or stator voltage measurements are needed. The feedback for the control is from the inverter output current, the DC-link voltage, and the rotor speed. The control method is further developed to obtain a speed-sensorless control method in Publications II and III. A speed-adaptation mechanism is proposed to be used with a full-order observer. The speed adaptation is based on the estimation error of the inverter output current. The adaptation law and the observer gain can be designed using a quasi-steady-state analysis and a linearization analysis. In Publication III, a field-weakening control method is proposed to enable operation at high speeds. When an LC filter is used, the maximum inverter output current and the maximum stator current are defined separately. These current limits and the voltage capability of the inverter are taken into account in field weakening. The control methods used in Publications I–III are explained in more detail in the following section.

3.3 Proposed Control Methods

Cascade Control

Fig. 3.3 shows a simplified block diagram of the control system, which is proposed in Publication II. The estimated quantities are marked by the symbol $\hat{}$. The angle of the estimated rotor flux, denoted by $\hat{\theta}_s$, is obtained by integrating the angular frequency $\hat{\omega}_s$ of

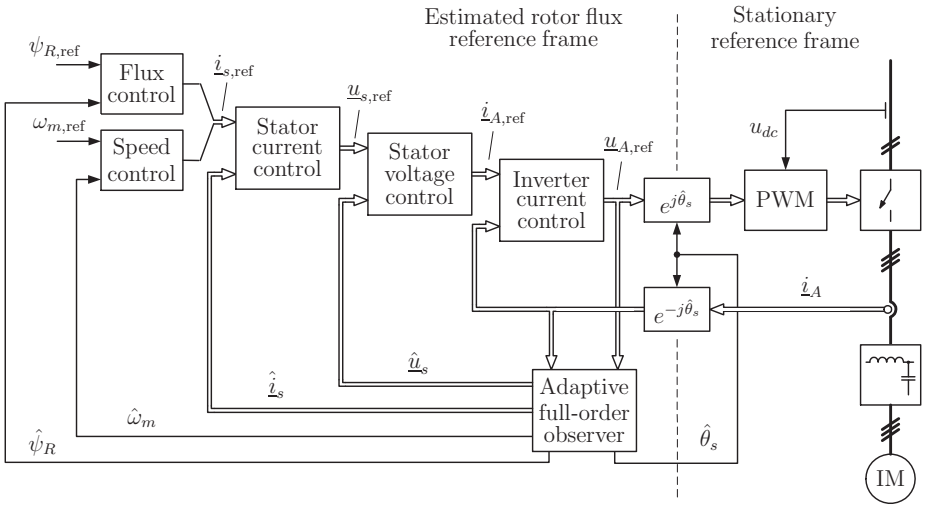

Figure 3.3. Simplified block diagram of cascade control system. Space vectors on the left-hand side of coordinate transformations are in the estimated rotor flux reference frame and on the right-hand side in the stationary reference frame. Double lines indicate complex quantities (space vectors) whereas single lines indicate real quantities (scalars).

the estimated rotor flux. The cascade control and the speed-adaptive full-order observer are implemented in the estimated rotor flux reference frame, where $\omega_k = \hat{\omega}_s$ and $\underline{\hat{\psi}}_R = \hat{\psi}_R + j0$.

The innermost control loop in Fig. 3.3 governs the inverter output current $\underline{i}_A$ by means of a PI controller. The stator voltage $\underline{u}_s$ is governed by a P or PI controller in the next control loop. The P controller was used in Publications I and II, but to avoid a steady-state error in the stator voltage, the PI controller was used in Publication III.

The motor control forms the outermost control loops: the stator current and the rotor speed are controlled by PI controllers. The output of the speed controller is the q-axis stator current reference. The rotor flux is controlled by a PI controller in Publications I and II. The estimated rotor flux is compared to the rotor flux reference, and the output of the controller is the d-axis stator current reference. Field weakening can be implemented by controlling the rotor flux inversely proportional to the rotor speed. Alternatively, the rotor flux can be regulated by an I-type voltage controller as reported in Publication III. The d-axis stator current reference is decreased if the unlimited inverter output voltage reference exceeds the maximum inverter output voltage. The advantage of the voltage controller is that it provides full utilization of the DC-link voltage automatically.

The control design is discussed in Publication II. The outer control loops can be designed by assuming ideal inner-loop controllers. However, better control performance is achieved by approximating the inner control loops with a first-order system when designing the outer-loop controller. Cross-couplings caused by the rotating reference frame are compensated, and a back-calculation method is used to avoid integrator windup.

Full-Order Observer

Most of the control methods reviewed in Section 3.2 are based on additional current or voltage measurements. However, no extra hardware should be added to the system, and the drive should preferably work without a speed sensor. In Publication I, a full-order observer is proposed for IM drives with an inverter output LC filter, which allows the vector control without additional current or voltage measurements. Because the stator current is not measured, the inverter output current is the feedback for the observer. The observer is defined by

$$\frac{d\hat{\mathbf{x}}}{dt} = \underline{\mathbf{A}}\,\hat{\mathbf{x}} + \mathbf{B}\underline{u}_A + \underline{\mathbf{K}}(\underline{i}_A - \hat{\underline{i}}_A) \tag{3.12}$$

where the observer gain vector is

$$\underline{\mathbf{K}} = \begin{bmatrix} \underline{k}_1 & \underline{k}_2 & \underline{k}_3 & \underline{k}_4 \end{bmatrix}^T. \tag{3.13}$$

Two different ways to select the observer gain $\underline{\mathbf{K}}$ for a speed-sensored drive are compared in Publication I. The first one is a pole placement method, where the observer gain varies with the rotor speed. In practice, gain scheduling is used: the observer gain is calculated in advance as a function of ω_m, and interpolation between tabulated values is used during the operation. The other proposed observer gain is a constant gain of the form

$$\underline{\mathbf{K}} = \begin{bmatrix} k_1 & 0 & 0 & 0 \end{bmatrix}^T \tag{3.14}$$

where k_1 is a real-valued gain parameter. According to experiments, the pole placement method and the constant gain method give similar results, and thus it is recommended to use a constant gain because it is easier to implement.

The saturation of the magnetizing inductance L_M may deteriorate the observer performance. The measured saturation characteristic can be used to improve the performance of the observer and the cascade control.

Speed Adaptation

The observer equation (3.12) contains the rotor angular speed in the system matrix $\underline{\mathbf{A}}$. If speed-sensorless operation is required, an adaptation mechanism can be used to estimate the rotor speed. The speed adaptation is a popular method for speed-sensorless drives without a filter (Schauder, 1992; Kubota et al., 1993; Yang and Chin, 1993; Maes and Melkebeek, 2000; Suwankawin and Sangwongwanich, 2002; Hinkkanen, 2004a). In Publications II and III, the speed adaptation is proposed for IM drives equipped with an LC filter. The conventional adaptation law cannot be used, because the stator current is not measured. The estimation error of the inverter output current is used instead of the usual estimation error of the stator current. The speed-adaptation law in the estimated rotor flux reference frame is

$$\begin{aligned} \hat{\omega}_m = &- K_p\, \mathrm{Im}\{(\underline{i}_A - \hat{\underline{i}}_A)e^{-j\phi}\} \\ &- K_i \int \mathrm{Im}\{(\underline{i}_A - \hat{\underline{i}}_A)e^{-j\phi}\}dt \end{aligned} \tag{3.15}$$

where K_p and K_i are nonnegative adaptation gains, and the angle ϕ changes the direction of the error projection. The change of the error projection is needed to stabilize the adaptive full-order observer at low speeds in a fashion similar to (Hinkkanen and Luomi, 2004) for the stator current. Quasi-steady-state analysis is used to visualize the selection of ϕ in Publications II and III.

Gain Selection for Speed-Adaptive Full-Order Observer

The observer gain $\underline{\mathbf{K}}$ affects the stability of the speed-adaptive full-order observer and it should be selected carefully. In Publication II, a simple observer gain (3.14) is used. According to linearization analysis, the observer is stable in a wide operation range. At higher speeds, however, the damping of the dominant poles is poor as shown in Publication III. An improved observer gain is proposed in Publication III:

$$\underline{\mathbf{K}} = \begin{bmatrix} k_1 & 0 & 0 & \lambda\{-1 + j\,\mathrm{sign}(\hat{\omega}_m)\} \end{bmatrix}^T \tag{3.16}$$

where

$$\lambda = \begin{cases} \lambda' \frac{|\hat{\omega}_m|}{\omega_\lambda}, & \text{if } |\hat{\omega}_m| < \omega_\lambda \\ \lambda', & \text{if } |\hat{\omega}_m| \geq \omega_\lambda \end{cases} \tag{3.17}$$

The positive constants λ' and ω_λ can be selected based on the linearization analysis. The damping of the dominant poles is increased, and the drive also operates well at higher speeds.

3.4 Performance Comparison With and Without an LC Filter

Cascade Control

A drive equipped with an LC filter needs two additional control loops as compared to a drive without a filter. The bandwidth of the innermost controller is determined according to the sampling frequency. Therefore, the bandwidth of the inverter output current control can be equal to the bandwidth of the stator current control of a drive without a filter. The cascade control requires an adequate bandwidth between each control loop, which causes a decreased bandwidth of the stator current control as compared to a drive without a filter. Therefore, the use of an LC filter is expected to slow down the dynamics of the stator current control.

In the following experimental comparison, a 2.2-kW IM drive was controlled in torque mode operation with and without an LC filter. When an LC filter was used, the sensorless vector control was that proposed in Publication III. The LC filter was the same used in Publication V ($L_f = 5.1$ mH, $C_f = 6.8$ µF). The bandwidths of the controllers were $2\pi \cdot 600$ rad/s for the inverter output current, $2\pi \cdot 400$ rad/s for the stator voltage, and $2\pi \cdot 200$ rad/s for the stator current. The parameters of the observer gain were $k_1 = 2000$ s^{-1}, $\lambda' = 10$ V/A and $\omega_\lambda = 1$ p.u. The parameters used in the speed adaptation were $K_p = 10\ (\mathrm{A \cdot s})^{-1}$ and $K_i = 10000\ (\mathrm{A \cdot s^2})^{-1}$. The sensorless vector control of the IM drive without a filter was based on (Hinkkanen, 2004a). The bandwidth of the stator current controller was $2\pi \cdot 600$ rad/s. Like in all experiments in this thesis, the parameter errors of the filter and the motor were kept as small as possible.

Fig. 3.4 shows d and q components of the stator current with and without an LC filter. A constant speed $\omega_m = 2\pi \cdot 25$ rad/s was maintained by a servo motor, and nominal torque reference was set for the IM drive at $t = 0.01$ s. When an LC filter is used, the rise time (from 10% to 90%) of i_{sq} is 2.7 ms. When an LC filter is not used, the rise time of i_{sq} is 0.5 ms. As was expected, the response of the stator current controller is slower when an LC filter is used than when it is not. However, most AC drive applications do not need very fast

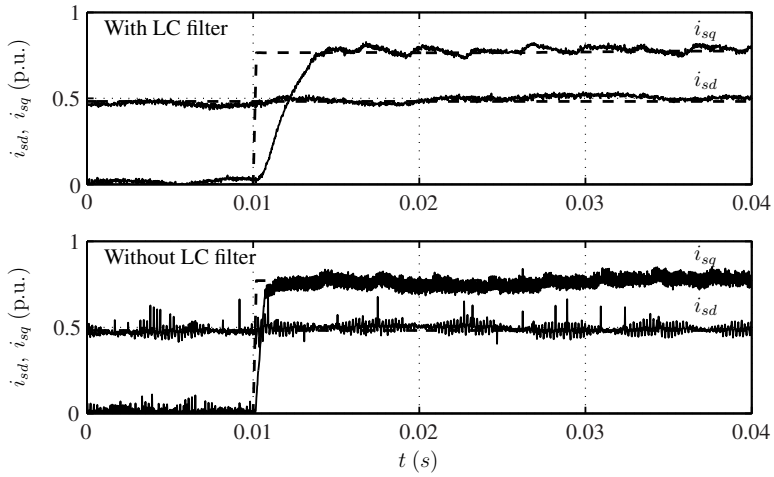

Figure 3.4. Experimental performance comparison of stator current control with and without LC filter. The solid lines are actual currents and dashed lines are reference values.

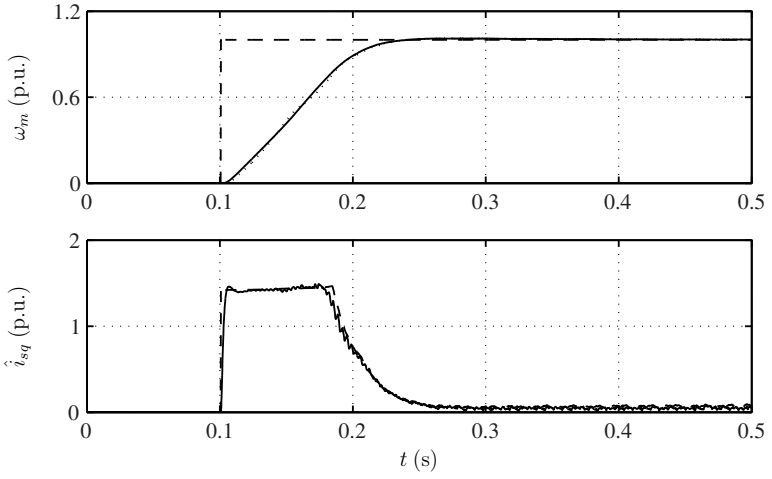

Figure 3.5. Experimental results showing acceleration from zero speed to 1 p.u. when LC filter is used. The first subplot shows the rotor speed (solid) and its reference (dashed). The second subplot shows q components of the stator current estimate (solid) and the stator current reference (dashed).

stator current control. Fast dynamics is important mainly in servo drives. The switching ripple is clearly seen in the lower subplot of Fig. 3.4. This ripple is reduced when an LC filter is added to the inverter output.

The bandwidth of the speed controller is usually well below the bandwidth of the stator current controller. Thus, the output filter is not expected to slow down the dynamics of the speed control. Fig. 3.5 shows experimental results obtained for an acceleration from zero speed to 1 p.u. The speed controller bandwidth was $2\pi \cdot 7.5$ rad/s and the stator current limit was 1.5 p.u. As can be seen in Fig. 3.5, the stator current is at its limit during the acceleration. Similar results were obtained when using an IM drive without an LC filter. The acceleration times were approximately equal in both drives.

Observer

The observer performance of speed sensorless drives can be evaluated by finding the minimum stator frequency where the system remains stable under load. Fig. 3.6 shows low-speed operation of a 2.2-kW IM drive equipped with an LC filter ($L_f = 5.1$ mH, $C_f = 6.8$ µF). The drive was controlled in the speed mode. The speed reference was set to 0.04 p.u. After applying a negative rated load torque the drive operates in the regenerating mode. The speed-adaptive observer remains stable even though the stator frequency is only $\omega_s = 0.009$ p.u. A similar experiment has been done by Hinkkanen and Luomi (2004) using a 2.2-kW IM drive without an LC filter. According to the experiment shown in Fig. 3.6 and several simulation and experimental results in Publications II–III, the speed-adaptive full-order observer works properly, and the performance is close to that of a drive without an LC filter. Parameter errors in the stator resistance, the filter resistance, and the inverter model have significant effects on the speed sensorless operation at low speeds. Parameter errors in the filter inductance and capacitance have only a minor effect on the stability of the system.

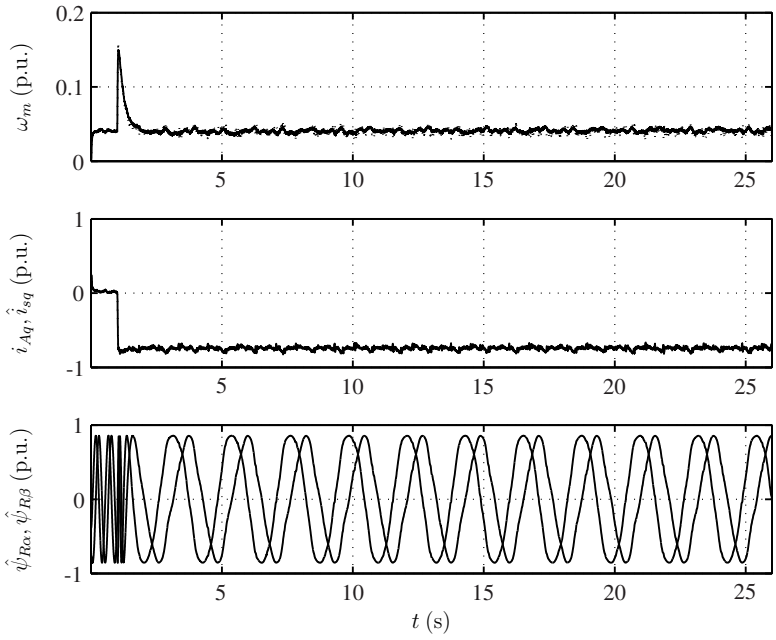

Figure 3.6. Experimental results showing low-speed operation when LC filter is used. The first subplot shows the rotor speed (solid) and its estimate (dotted). The second subplot shows the q components of the stator current estimate (solid) and inverter output current (dotted). The third subplot shows the real and imaginary components of the rotor flux estimate in the stationary reference frame.

Chapter 4

Control of PMSM Drives Equipped With an LC Filter

Inverter output filters are mostly used in induction motor drives. However, problems caused by the pulse-width-modulated voltage have also been reported on for permanent magnet synchronous motors (Carpita et al., 2001b; Batzel and Lee, 2005; Yamazaki and Seto, 2006). In this chapter, the system model is presented for a three-phase LC filter and a PMSM, after which state-of-the-art control methods are reviewed for such a system. Finally, the cascade control structure, the full-order observer, and the speed adaptation mechanism proposed in this thesis are presented.

4.1 System Model

The space vector notation used in connection with induction motor drives is inconvenient for modeling permanent magnet motors with magnetic saliency. Therefore, matrix notation is preferred in PMSM drives. Fig. 4.1 shows a drive system consisting of a frequency converter, LC filter, and PMSM. The inverter output voltage $\mathbf{u}_A$ is filtered by an LC filter, and the PMSM is fed by the filtered voltage $\mathbf{u}_s$. The inverter output current and the stator current are denoted by $\mathbf{i}_A$ and $\mathbf{i}_s$, respectively.

In a reference frame rotating at electrical angular speed ω_m of the rotor, the equations of the LC filter are

$$\frac{d\mathbf{i}_A}{dt} = -\frac{R_{Lf}}{L_f}\mathbf{i}_A - \omega_m \mathbf{J}\mathbf{i}_A + \frac{1}{L_f}(\mathbf{u}_A - \mathbf{u}_s) \tag{4.1}$$

$$\frac{d\mathbf{u}_s}{dt} = -\omega_m \mathbf{J}\mathbf{u}_s + \frac{1}{C_f}(\mathbf{i}_A - \mathbf{i}_s), \tag{4.2}$$

where $\mathbf{i}_A = \begin{bmatrix} i_{Ad} & i_{Aq} \end{bmatrix}^T$ is the inverter output current, $\mathbf{u}_A = \begin{bmatrix} u_{Ad} & u_{Aq} \end{bmatrix}^T$ the inverter output voltage, $\mathbf{u}_s = \begin{bmatrix} u_{sd} & u_{sq} \end{bmatrix}^T$ the stator voltage, $\mathbf{i}_s = \begin{bmatrix} i_{sd} & i_{sq} \end{bmatrix}^T$ the stator current, and

$$\mathbf{J} = \begin{bmatrix} 0 & -1 \\ 1 & 0 \end{bmatrix}$$

In the d-q reference frame fixed to the rotor, the voltage equation of the PMSM is

$$\mathbf{u}_s = R_s \mathbf{i}_s + \frac{d\boldsymbol{\psi}_s}{dt} + \omega_m \mathbf{J}\boldsymbol{\psi}_s \tag{4.3}$$

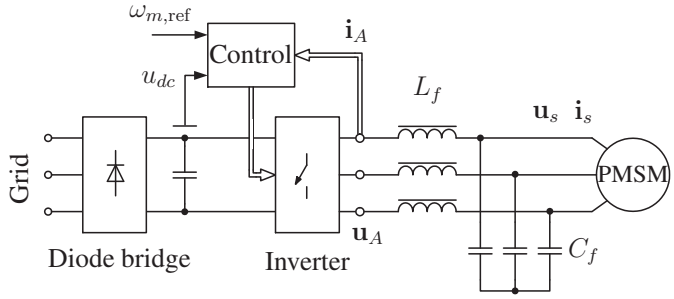

Figure 4.1. Permanent magnet synchronous motor (PMSM) drive equipped with three-phase LC filter.

where R_s is the stator resistance. The stator flux linkage is

$$\boldsymbol{\psi}_s = \mathbf{L}_s \mathbf{i}_s + \boldsymbol{\psi}_{pm} \tag{4.4}$$

where $\boldsymbol{\psi}_{pm} = \begin{bmatrix} \psi_{pm} & 0 \end{bmatrix}^T$ is the permanent magnet flux linkage. The stator inductance matrix

$$\mathbf{L}_s = \begin{bmatrix} L_d & 0 \\ 0 & L_q \end{bmatrix}$$

consists of the direct-axis inductance L_d and quadrature-axis inductance L_q. The electromagnetic torque is

$$T_e = \frac{3p}{2} \boldsymbol{\psi}_s^T \mathbf{J}^T \mathbf{i}_s \tag{4.5}$$

where p is the number of pole pairs.

Based on Eqs. (4.1)–(4.4), the state-space representation of the system can be written as

$$\frac{d\mathbf{x}}{dt} = \underbrace{\begin{bmatrix} -R_{Lf} L_f^{-1} \mathbf{I} - \omega_m \mathbf{J} & -L_f^{-1} \mathbf{I} & \mathbf{0} \\ C_f^{-1} \mathbf{I} & -\omega_m \mathbf{J} & -C_f^{-1} \mathbf{L}_s^{-1} \\ \mathbf{0} & \mathbf{I} & -R_s \mathbf{L}_s^{-1} - \omega_m \mathbf{J} \end{bmatrix}}_{\mathbf{A}} \mathbf{x} + \underbrace{\begin{bmatrix} L_f^{-1} \mathbf{I} & \mathbf{0} \\ \mathbf{0} & C_f^{-1} \mathbf{L}_s^{-1} \\ \mathbf{0} & R_s \mathbf{L}_s^{-1} \end{bmatrix}}_{\mathbf{B}} \begin{bmatrix} \mathbf{u}_A \\ \boldsymbol{\psi}_{pm} \end{bmatrix} \tag{4.6}$$

$$\mathbf{i}_A = \underbrace{\begin{bmatrix} \mathbf{I} & \mathbf{0} & \mathbf{0} \end{bmatrix}}_{\mathbf{C}} \mathbf{x} \tag{4.7}$$

where $\mathbf{x} = \begin{bmatrix} \mathbf{i}_A^T & \mathbf{u}_s^T & \boldsymbol{\psi}_s^T \end{bmatrix}^T$ is the state vector and $\mathbf{I}$ is a 2×2 identity matrix. The inverter output voltage $\mathbf{u}_A$ and the permanent magnet flux linkage $\boldsymbol{\psi}_{pm}$ are considered as inputs to the system.

4.2 Control Structures

There are only a few publications that deal with the control of synchronous motor drives equipped with an LC filter. Different output filter topologies have been tested on a 25-hp PMSM drive by Sozer et al. (2000). A field-oriented control method is used, but it is

not documented in detail. The measurements needed for the control are the stator current, the rotor speed, and the DC-link voltage. A predictive current control is implemented to provide stable operation despite the filter.

Carpita et al. (2001b) have investigated two different methods to compensate for the effects of an LC filter in sensorless high-speed PMSM drives. In both methods, the rotor position is estimated by means of a modified voltage model (Carpita et al., 2001a). The first method uses feed-forward voltage terms that are based on the approximated system equations. The feed-forward terms are added to the output of the stator current controller. The method requires measurements of the stator voltage and the stator current. The other investigated method presented by Carpita et al. (2001b) is based on sliding mode control. The switching functions are determined according to the error vector consisting of the difference between the stator voltage and its reference and the difference between the derivative of the stator voltage and its reference. The control method requires measurements of the capacitor current, the stator voltage, and the stator current. According to simulation results, both control methods work well.

Batzel and Lee (2005) have used a sensorless control method for PMSM drives equipped with an LC filter. Originally, the control method was developed for a drive without a filter at the inverter output. A voltage-model-based speed estimate is enhanced by an adaptive speed estimate in a fashion similar to (Kim and Sul, 1997b). When an LC filter is used, the method requires measurements of the stator current and the stator voltage, and no modifications are made to the control due to the LC filter. The measured stator voltage is low-pass filtered causing an unwanted time delay. The experimental results obtained using a 70-hp PMSM show an adequate performance at high speeds, but the low-speed operation at start-ups and reversals is problematic.

Park et al. (2005) have presented a feed-forward current controller in a speed-sensored synchronous reluctance motor drive with an LC filter. The effects of the LC filter are compensated for by using a filter model. Even though feed-forward current control is used, the stator current and the DC-link voltage are measured. The experimental results with a 120-kW synchronous reluctance motor drive confirm the reduction of losses in the motor due to the LC filter.

Szczupak and Pacas (2006) have used cascaded controllers and a full-order observer for a PMSM drive equipped with an LC filter. The control method is based on Publication I, and it requires measurements of the inverter output current and the rotor speed. The main focus in the paper is on the identification of the system parameters.

Publication V proposes a sensorless control method that does not need additional measurements due to the LC filter. An adaptive full-order observer is used to estimate the stator voltage, the stator current, the rotor speed, and the rotor position. The observer is analyzed and tuned using a linearized model.

The high speed performance of the sensorless PMSM drive equipped with an LC filter is enhanced in Publication VI. The influence of the filter on the theoretical maximum torque and speed is investigated. The proposed field-weakening method based on voltage control enables the maximum-torque operation at high speeds.

In Publication VII, the adaptive full-order observer is combined with a signal injection method allowing sustained operation down to zero speed. It is shown that the signal injection method can be used for the rotor speed and position estimation even if an LC filter is connected between the inverter and the motor. The control methods proposed in Publications V−VII are explained in more detail in the following section.

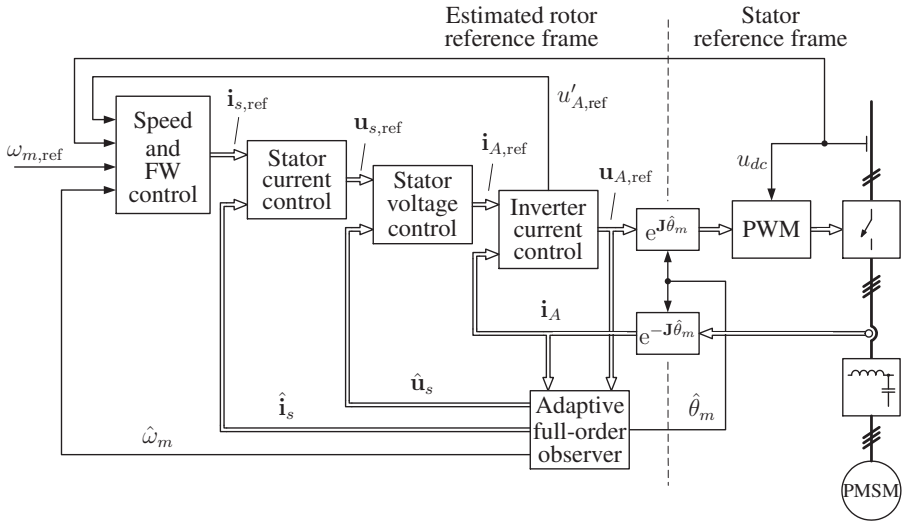

Figure 4.2. Simplified block diagram of the cascaded control system. Double lines indicate vector quantities whereas single lines indicate scalar quantities.

4.3 Proposed Control Methods

Fig. 4.2 shows a simplified block diagram of the control system used in Publication VI. The control is implemented in the estimated rotor reference frame. The inverter output current, the stator voltage, and the stator current are controlled by PI controllers, and cross-couplings due to the rotating reference frame are compensated. An adaptive full-order observer is used to estimate unmeasured system states making it possible to avoid additional measurements due to the LC filter. The field weakening (FW) starts when the unlimited inverter output voltage reference $u'_{A,\mathrm{ref}}$ exceeds the maximum inverter output voltage. The field-weakening control was not used in Publication V.

Speed-Adaptive Full-Order Observer

A speed-adaptive full-order observer for PMSM drives equipped with an LC filter was proposed in Publication V. The inverter output current is a feedback signal for the observer, and the electrical angular speed of the rotor is estimated using an adaptation mechanism. The observer is defined by

$$\frac{d\hat{\mathbf{x}}}{dt} = \hat{\mathbf{A}}\,\hat{\mathbf{x}} + \mathbf{B}\begin{bmatrix}\mathbf{u}_A \\ \hat{\boldsymbol{\psi}}_{pm}\end{bmatrix} + \mathbf{K}(\mathbf{i}_A - \hat{\mathbf{i}}_A) \tag{4.8}$$

where $\mathbf{K}$ is the observer gain and the system matrix is

$$\hat{\mathbf{A}} = \begin{bmatrix} -R_{Lf}L_f^{-1}\mathbf{I} - \hat{\omega}_m\mathbf{J} & -L_f^{-1}\mathbf{I} & \mathbf{0} \\ C_f^{-1}\mathbf{I} & -\hat{\omega}_m\mathbf{J} & -C_f^{-1}\mathbf{L}_s^{-1} \\ \mathbf{0} & \mathbf{I} & -R_s\mathbf{L}_s^{-1} - \hat{\omega}_m\mathbf{J} \end{bmatrix} \tag{4.9}$$

The adaptation law is

$$\hat{\omega}_m = -K_p\,(i_{Aq} - \hat{i}_{Aq}) - K_i \int (i_{Aq} - \hat{i}_{Aq})dt \tag{4.10}$$

where K_p and K_i are nonnegative adaptation gains. The estimated rotor position $\hat{\theta}_m$ is obtained by integrating the estimated rotor speed $\hat{\omega}_m$. Publication V deals with the linearization analysis and the observer gain selection. In order to have a locally stable observer in a wide speed range, the observer gain

$$\mathbf{K} = \begin{bmatrix} k_{1d}\mathbf{I} \\ \mathbf{0} \\ k_{3d}\mathbf{I} + k_{3q}\mathrm{sign}(\hat{\omega}_m)\mathbf{J} \end{bmatrix} \tag{4.11}$$

is proposed. The gain parameters k_{1d}, k_{3d}, and k_{3q} are positive constants.

According to the experiments with a 2.2-kW PMSM drive, the sensorless control method based on the speed-adaptive full-order observer works well down to speed 0.07 p.u. At lower speeds under load, the system becomes unstable due to the inverter nonidealities and the inaccuracies of the motor parameters. At no load, the system is stable down to zero speed.

Field-Weakening Control

The DC-link voltage constrains the inverter output voltage. In order to reach high speeds, the magnetic field must be weakened by supplying negative d-axis stator current. The maximum torque is limited by the maximum allowable current. When an LC filter is used, the inverter output current and the stator current can be limited separately. The influence of an LC filter on the maximum torque and speed of PMSM drives is investigated in Publication VI. In addition, a field-weakening method based on voltage control is proposed. Voltage control has been successfully used in IM and PMSM drives that are not equipped with an LC filter (Kim and Sul, 1997c,a; Harnefors et al., 2001).

The field weakening is implemented by adding an incremental d-axis stator current reference $i_{sd\Delta}$ to the d-axis current reference $i_{sd\mathrm{M}}$ that is in accordance with the maximum torque-per-ampere (MTPA) trajectory. The d-axis current reference is thus

$$i_{sd,\mathrm{ref}} = i_{sd\mathrm{M}} + i_{sd\Delta} \tag{4.12}$$

The voltage control algorithm is

$$\frac{di_{sd\Delta}}{dt} = \gamma_f \left[u_{A,\max}^2 - (u'_{A,\mathrm{ref}})^2 \right], \quad i_{sd\Delta,\min} \leq i_{sd\Delta} \leq 0 \tag{4.13}$$

where γ_f is the controller gain, $u_{A,\max}$ is the maximum inverter output voltage, and $u'_{A,\mathrm{ref}}$ is the magnitude of the unlimited inverter output voltage reference. The lower limit of $i_{sd\Delta}$ is designed as

$$i_{sd\Delta,\min} = -i_{sd\mathrm{M}} + \max\left\{ -i_{s,\max}, \frac{i_{A,\max} - \hat{\omega}_m^2 C_f \psi_{pm}}{\hat{\omega}_m^2 C_f L_d - 1} \right\} \tag{4.14}$$

where $i_{s,\max}$ and $i_{A,\max}$ are the maximum allowable stator and inverter output currents, respectively. The second term inside the maximum function is based on a steady-state solution of (4.6) assuming $R_s = 0$. It prevents the violation of the inverter output current limit.

The q-axis stator current reference is limited according to

$$i_{sq,\mathrm{ref}} = \mathrm{sign}(i'_{sq,\mathrm{ref}}) \cdot \min\Bigg\{ |i'_{sq,\mathrm{ref}}|, \sqrt{i^2_{s,\max} - i^2_{sd,\mathrm{ref}}}\,, \frac{\sqrt{i^2_{A,\max} - \left[(\hat{\omega}_m^2 C_f L_d - 1) i_{sd,\mathrm{ref}} + \hat{\omega}_m^2 C_f \psi_{pm}\right]^2}}{1 - \hat{\omega}_m^2 L_q C_f} \Bigg\} \quad (4.15)$$

The minimum of the three values is chosen: (i) the absolute value of the unlimited reference $i'_{sq,\mathrm{ref}}$; (ii) the value defined by the maximum stator current; or (iii) the value defined by the maximum inverter output current assuming $R_s = 0$. The experiments with a 2.2-kW PMSM drive show that the proposed field-weakening method works well both in steady and transient states.

Signal Injection

Signal injection methods make use of the magnetic asymmetry, i.e. saliency, of motors for estimating the rotor position. Interior permanent magnet synchronous motors (IPMSMs) have the magnets mounted inside the rotor resulting in saliency. In Publication VII, the sustained operation at low speeds is made possible by augmenting the adaptive full-order observer with a signal injection method. The high-frequency signal injection is based on a method developed by Corley and Lorenz (1998). The combination of the high-frequency signal injection method and the adaptive full-order observer has been developed by Piippo and Luomi (2005) for PMSM drives without an LC filter.

A carrier excitation signal $\hat{u}_c \cos(\omega_c t)$, having amplitude $\hat{u}_c$ and angular frequency ω_c, is superimposed on the d-axis inverter output voltage reference in the estimated rotor reference frame. A response is detected on the q-axis inverter output current, from which an error signal ε, proportional to the rotor position estimation error, can be extracted:

$$\varepsilon = \mathrm{LPF}\Big\{ \mathrm{BPF}\big\{ i_{Aq} \big\} \sin(\omega_c t) \Big\} \quad (4.16)$$

Here, LPF means low-pass filtering and BPF means band-pass filtering. In a conventional signal injection, when an inverter output filter is not used, the excitation signal is superimposed on the stator voltage reference and detected on the stator current.

A correction term ω_ε for the estimated rotor speed $\hat{\omega}_m$ is obtained using a PI mechanism

$$\omega_\varepsilon = \gamma_p \varepsilon + \gamma_i \int \varepsilon dt \quad (4.17)$$

where γ_p and γ_i are nonnegative gains. The correction term is used by replacing $\hat{\omega}_m$ in (4.9) with $\hat{\omega}_m - \omega_\varepsilon$.

The signal injection is not needed at higher speeds, so its influence is reduced as the rotor speed increases. Both the HF excitation voltage $\hat{u}_c$ and the approximate bandwidth of the PI mechanism in (4.17) are linearly decreased as the speed increases, reaching zero at the transition speed ω_Δ. The experimental results, presented in Publication VII, show that the sensorless PMSM drive equipped with an LC filter can stand nominal load torque steps even at zero speed.

Chapter 5

Experimental Setup

The experimental setup used in this thesis is described in this chapter. In Publications I–IV and VIII, the investigated motor was a standard 2.2-kW induction motor. In Publications V and VI, the investigated motor was an experimental 2.2-kW permanent magnet synchronous motor.

Fig. 5.1 shows an overview of the experimental setup. The investigated motor (IM or PMSM) is supplied by a VLT5004 frequency converter through an inverter output filter. The motor is loaded by a PM servo motor driven by a Bivector frequency converter. Both frequency converters are equipped with braking resistors (BR). The system is controlled by a dSPACE DS1103 PCC/DSP board connected to a PC. A photograph of the experimental setup is shown in Fig. 5.2. The technical data of the hardware is given in Table 5.1. The parameters of the 2.2-kW IM and 2.2-kW PMSM are given in Tables 5.2 and 5.3, respectively.

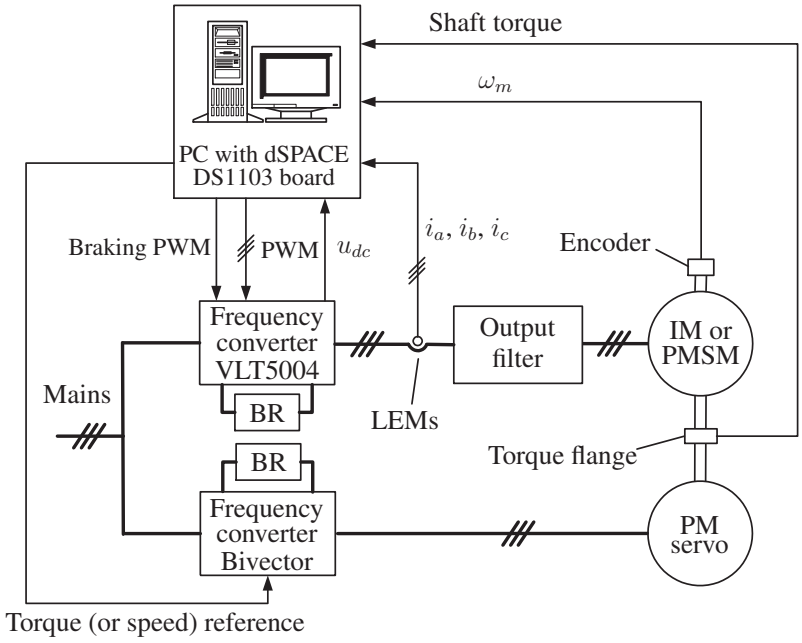

Figure 5.1. Experimental setup.

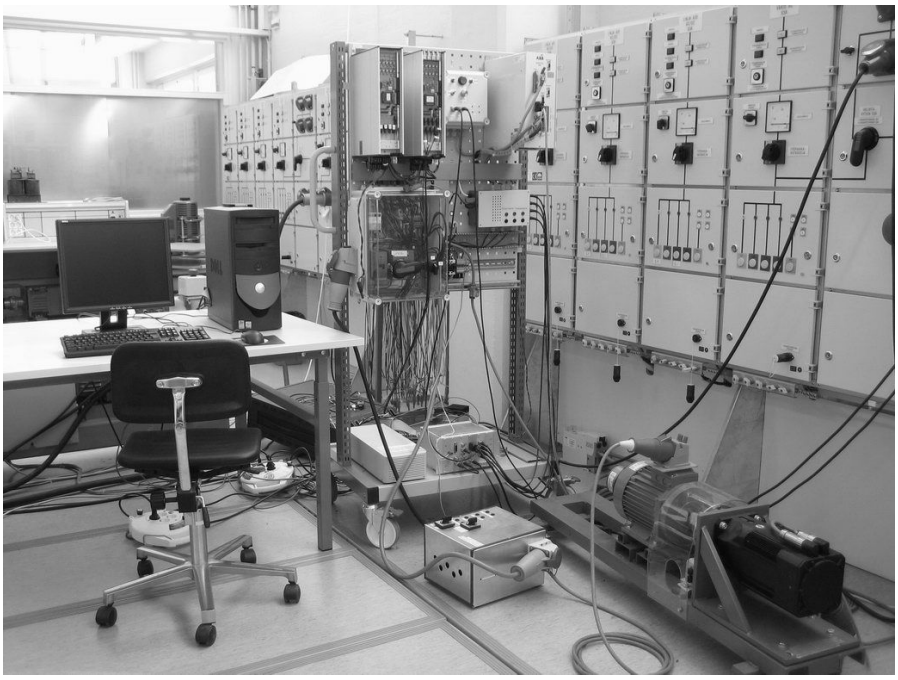

Figure 5.2. Photograph of experimental setup.

The technical data of the LC filter used in each publication are given in Table 5.4. In Publications I−III, the capacitors of the LC filter were in delta connection. In Publication IV, a sinusoidal DM and CM filter similar to that shown in Fig. 2.11 was built. The CM inductor was built using two toroidal VITROPERM cores and three windings with 24 turns in each. The DM part of the filter was used in Publications V−VII. All three-phase inductors used in the experiments were laminated iron-core inductors.

The original VLT5004 frequency converter was modified in order to control the gate signals directly from the dSPACE DS1103 PCC/DSP board. The original controller board of the frequency converter was replaced with an interface and protection board compatible with the DS1103 board. This hardware modification was developed at Aalborg University in Denmark (Teodorescu et al., 2000). The feedback signals from the phase currents, the DC-link voltage, and the motor speed are connected to the DS1103 board through a signal conditioning unit. The braking choppers connected to the VLT5004 are also controlled by the DS1103 board. An analogue torque (or speed) reference was provided by the DS1103 board for the Bivector frequency converter that supplies the servo motor. The shaft torque was measured using a HBM T10F torque flange for monitoring purposes.

The developed control algorithms were programmed using the MATLAB/Simulink software. The Simulink Real-Time Workshop generates an executable C-code from the Simulink model, after which the dSPACE Real-Time Interface builds and downloads the code to the DS1103 board. The program execution can be monitored and controlled using the dSPACE ControlDesk software. The pulse-width modulation was generated by the slave DSP of the DS1103 board. The sampling frequency was equal to the switching frequency of 5 kHz in all experiments in this thesis.

Table 5.1. Technical data of the experimental setup.

Induction motor	ABB M2AA 100LA 3GAA102001-ADA
Rating plate	380...420 V, 50 Hz, 1 430 r/min, 2.2 kW, 5.0 A, $\cos\varphi = 0.81$
Moment of inertia	0.0069 kgm^2
Permanent magnet synchronous motor	ABB M2BJ 100L 6B3
Rating plate	370 V, 75 Hz, 1 500 r/min, 2.2 kW, 4.3 A, $\cos\varphi = 0.90$
Frequency converter	Danfoss VLT5004 P T5 B20 EB R3 (modified)
Supply voltage	380...500 V (50/60 Hz)
Output voltage	0...100 % of supply voltage
Max. const. output current	5.6 A
Output frequency	0...1 000 Hz
PM servo motor	ABB 8C5 230 00YA02SL3MB
Rating plate	315 V, 3 000 r/min, cont. stall torque 21.5 Nm (14.1 A), peak stall torque 75.3 Nm (54.6 A)
Moment of inertia	0.0040 kgm^2
Frequency converter for PM servo	ABB Bivector 535 "25"
Rated supply voltage	400 V (50/60 Hz)
Rated output voltage	400 V
Rated cont. output current	25.0 A
Current transducers	LEM LA 55-P/SP1
Bandwidth	0...200 kHz (-1 dB)
Accuracy (at 25°C, rated current)	± 0.9 %
Incremental encoder	Leine & Linde 186 90311
Line counts	2 048 ppr
Moment of inertia	$42 \cdot 10^{-6}$ kgm^2
Torque transducer	HBM K-T10F-050Q-SU2-G-1-W1-Y
Rated torque	50 Nm
Maximum speed	15 000 r/min
Torsional stiffness	160 kNm/rad
Bandwidth	0...1 kHz (-3 dB)
Moment of inertia	0.0017 kgm^2
Coupling	HBM BSD-MODULFLEX for K-T10F
Torsional stiffness	24 kNm/rad
Moment of inertia (incl. joint)	0.0029 kgm^2
Controller board	dSPACE DS1103 PPC
Master processor	PowerPC 604e (400 MHz, 2 MB local SRAM, 128 MB global DRAM)
Slave processor	Texas Instruments TMS320F240 DSP (20 MHz, 3-phase PWM generation)

Table 5.2. Parameters of 2.2-kW 4-pole 400-V 50-Hz IM and load.

Rated torque T_N	14.6 Nm
Stator resistance R_s	3.67 Ω
Rotor resistance R_R	2.10 Ω
Magnetizing inductance L_M	0.224 H
Stator transient inductance L'_s	0.0209 H
Total moment of inertia J	0.0155 kgm^2
Viscous friction coefficient	0.0025 Nm·s

Table 5.3. Parameters of 2.2-kW 6-pole 380-V 75-Hz PMSM and load.

Rated torque T_N	14.0 Nm
Stator resistance R_s	3.59 Ω
Direct-axis inductance L_d	36.0 mH
Quadrature-axis inductance L_q	51.0 mH
Permanent magnet flux linkage ψ_{pm}	0.545 Vs
Total moment of inertia J	0.015 kgm^2

Table 5.4. Technical data of inverter output filters.

Filter used in Publications I–III	
3-phase inductor	Platthaus UAG 941/16/8 Nr.:L122985
Inductance	3 x 8.0 mH
Rated voltage	690 V
Rated current	16 A
Rated frequency	50/60 Hz
Rated switching frequency	2/4 kHz
Capacitors	3 x VISHAY PEC-Kondensator KMKP 1100 -3.30 IA
Capacitance	3.3 µF ±10 % (9.9-µF per phase in delta connection)
Rated voltage	1100 V
Filter used in Publications IV–VII	
3-phase inductor	Block B0403092 3 LC Filter for ABB VFD ACS 800 Series (capacitors removed)
Inductance	3 x 5.10 mH
Voltage range	0-440/520 V
Frequency range	0-150 Hz
Rated current	10.0 A
Capacitor	3 x EPCOS B25834-L6685-K009 MKV
Capacitance	6.8 µF ±10 %
Rated voltage	900 V
CM filter used in Publication IV	
CM inductor	Core: 2 x Vacuumschmelze VITROPERM W631-52
Inductance	20 mH
Number of winding turns	24 (per phase)
Capacitor	VISHAY PEC-Kondensator KMKP 900 -2.2 IA
Capacitance	2.2 µF ±10 %
Rated voltage	900 V
Resistor	
Resistance	10 Ω
Filter used in Publication VIII	
3-phase inductor	Muuntosähkö Trafox 3INP5 50145
Inductance	3 x 4.0 mH
Rated voltage	400 V
Rated current	5.0 A
Capacitor	3 x EPCOS B25832-F4505-K001 MKV
Capacitance	5.0 µF ±10 %
Rated voltage	640 V

Chapter 6

Summary of Publications

Summaries of the publications which comprise this thesis are reprinted in Section 6.1. Publication I deals with speed-sensored control and Publications II and III with speed-sensorless control of IM drives equipped with an LC filter. In Publication IV, different PWM methods are compared when a sinusoidal differential-mode and common-mode filter is used. Publications V, VI, and VII deal with speed-sensorless control of PMSM drives equipped with an LC filter. Publication VIII focuses on the design of inverter output filters. The contribution of the thesis is described in Section 6.2.

6.1 Abstracts

Publication I

This paper introduces a control method for an induction motor that is supplied by a PWM voltage source inverter through an LC filter. A cascade control structure is employed and a full-order observer is used to estimate the system states. Thus no additional voltage or current measurements are needed for the vector control of the motor. Two alternative methods are presented for the observer gain selection. Simulation and experimental results confirm the functionality of the proposed control method.

Publication II

The paper presents a speed sensorless vector control method for an induction motor that is supplied by a PWM inverter through an output LC filter. The system states are estimated by an adaptive full-order observer, and no additional voltage, current or speed measurements are needed. The rotor speed adaptation is based on the estimation error of the inverter output current. Quasi-steady-state analysis is used to illustrate the speed adaptation, and the stability is analyzed using a linearized model. Simulation and experimental results show that it is possible to achieve performance comparable to that of a drive without the LC filter.

Publication III

This paper deals with the speed sensorless vector control of an induction motor in a special case where the output voltage of the PWM inverter is filtered by an LC filter. The system states are estimated by means of an adaptive full-order observer, and no additional voltage,

current or speed measurements are needed. The rotor speed adaptation is based on the estimation error of the inverter output current. Quasi-steady-state and linearization analyses are used to design an observer that enables a wide operation region, including very low and very high speeds. A torque-maximizing control method is applied in the field-weakening region. Simulation and experimental results show that the performance is comparable to that of a drive without the LC filter.

Publication IV

This paper deals with the suitability of various pulse-width modulation techniques for a variable-speed AC drive equipped with a sinusoidal differential-mode and common-mode filter at the inverter output. Simulations and experiments are used for the investigation. If the average common-mode voltage is changed abruptly, the filter resonance may be excited, and the common-mode voltage at the motor terminals may rise to values higher than those obtained without the filter. This phenomenon may cause difficulties when the modulation is started, and it also creates a fundamental problem when a two-phase modulation method is used. The resonance problem can be avoided by selecting a modulation technique that does not cause sudden changes in the average common-mode voltage. A starting algorithm is proposed, enabling a trouble-free start of the drive equipped with a sinusoidal common-mode filter.

Publication V

The paper presents a sensorless vector control method for a permanent magnet synchronous motor when the output voltage of the PWM inverter is filtered by an LC filter. The dynamics of the LC filter are taken into account in the design of the controller and adaptive full-order observer. The use of the output filter does not require additional current or voltage measurements. The speed adaptation is based on the estimation error of the inverter output current. Linearization analysis is used to design an observer that enables a wide operation region. Simulation and experimental results show the functionality of the proposed control method.

Publication VI

The paper deals with the maximum torque and speed of permanent magnet synchronous motor (PMSM) drives when the inverter output voltage is filtered by an LC filter with a cut-off frequency well below the switching frequency. According to steady-state analysis, the filter affects the performance of the motor drive especially at high speeds. The stator current is not equal to the inverter current, and due to the inverter current and inverter voltage limits, the torque-maximizing stator current locus differs from that of a drive without the filter. A field-weakening method is proposed for PMSM drives with an inverter output filter. The method is implemented and tested in a 2.2-kW PMSM drive. The experimental results agree well with the analysis, and validate the high-speed performance of the proposed field-weakening method.

Publication VII

The paper proposes a hybrid observer for sensorless control of permanent magnet synchronous motor drives equipped with an inverter output LC filter. An adaptive full-order observer is augmented with a high-frequency signal injection method at low speeds. The only measured quantities are the inverter phase currents and the DC-link voltage. It is shown that the LC filter is not an obstacle to using signal injection methods. The proposed method allows sensorless operation in a wide speed range down to zero speed. Experimental results are given to confirm the effectiveness of the proposed method.

Publication VIII

The paper deals with the minimization of output filter cost in inverter-fed AC drives. The LC filter design is constrained by the total harmonic distortions of the stator voltage and inverter output current, the voltage drop in the filter inductor, and the system resonance frequency. The last constraint is important from the control point of view, because the vector control requires that the sampling frequency is sufficiently higher than the resonance frequency. The design takes into account the frequency dependence of the filter resistance and inductance due to the eddy currents in the laminated iron-core inductor. The design method is further enhanced by taking into account the inverter power stage cost as a function of the switching frequency. The design minimizes the total cost of the inverter and filter, and determines the optimal switching frequency. Simulations and experiments show that the filter designed according to the proposed design procedure fulfils the design constraints, and the speed-sensorless control works well with the cost-optimized filter.

6.2 Contribution of the Thesis

The main contributions of the thesis can be summarized as follows:

- A full-order observer for IM drives equipped with an LC filter is proposed in Publication I. The observer estimates the stator voltage, the stator current, and rotor flux linkage, and therefore no additional measurements are needed for the vector control.
- In Publication II, a speed-adaptation mechanism is added to the full-order observer enabling speed-sensorless operation of IM drives equipped with an LC filter.
- A field weakening method based on a voltage control is proposed in Publication III for IM drives equipped with an LC filter. A similar voltage control algorithm has been used by Harnefors et al. (2001) without an LC filter.
- A speed and position sensorless control method based on a full-order observer and speed adaptation is proposed for PMSM drives equipped with an LC filter in Publication V.
- The influence of an inverter output LC filter on the maximum torque and speed of PMSM drives is analyzed and a new field weakening method is developed in Publication VI.
- In Publication IV, it is shown that the two-phase (or discontinuous) modulation method may excite the CM filter resonance and causes excessive oscillation in the

CM current if a sinusoidal CM filter is used at the inverter output. Symmetrical suboscillation or the corresponding space vector modulation (SVPWM) is suitable method when a sinusoidal CM filter is used. A starting algorithm is proposed to solve a starting problem originating from the saturated CM inductor.

- A high-frequency signal injection method combined with an adaptive full-order observer is jointly developed for PMSM drives equipped with an LC filter in Publication VII.
- An LC filter design method that minimizes the filter cost is proposed in Publication VIII. The method takes the vector control into account.

Chapter 7

Conclusions

In this thesis, new sensorless vector control methods are developed for IM and PMSM drives equipped with a sinusoidal LC filter at the inverter output. The innovation of the developed control methods is to use a full-order observer to estimate unmeasured state variables of the filter and the motor. A speed-adaptation mechanism enables speed and position sensorless operation. The control methods require only measurements of the inverter output current and the DC-link voltage. Thus, an LC filter can be added to an existing drive without any hardware modifications. Only changes in the control software of the frequency converter are needed.

First, a speed-sensored vector control method was developed for IM drives equipped with an LC filter. The full-order observer based on filter and motor equations estimates the stator voltage, the stator current, and the rotor flux linkage. The feedback is taken from the inverter output current. The observer gain can be selected by means of pole placement, but a constant gain gives similar results and is more convenient to use. Cascaded controllers for the inverter output current, the stator voltage, the stator current, and the rotor speed work well if they are carefully tuned.

Speed-sensorless operation of IM drives with an LC filter was made possible by adding a speed-adaptation mechanism to the observer. A PI-type adaptation mechanism is based on the estimation error of the inverter output current. The observer gain and adaptation parameters can be selected by means of quasi-steady-state and linearization analyses. According to experimental results, the speed-sensorless control method works well in wide speed and load ranges. However, inaccurate parameters and inverter nonidealities cause unstable operation at very low stator frequencies even if the system is stable according to the linearization analysis (marginally stable at zero frequency). The minimum stator frequency that can be reached under loaded conditions is approximately equal to that obtained for sensorless drives without a filter.

A sensorless vector control method was developed for PMSM drives equipped with an LC filter. The full-order observer is based on filter and motor equations, and a PI-type adaptation mechanism uses the estimation error of the inverter output current to adapt the rotor speed. Linearization analysis is a suitable method for designing an observer gain for the system. The stability problem at very low speeds under load can be solved by augmenting the adaptive observer with a signal injection method. Even if the filter is present, the signal injection method works properly. The sensorless PMSM drive equipped with an LC filter can stand nominal load torque steps even at zero speed.

When an LC filter is used the limits for the inverter output current and for the stator current can be defined separately. These current limits and the inverter output voltage

limit determine an optimal stator current locus for the maximum-torque operation. Depending on the current limits, the maximum torque can be even higher with an LC filter than without it. The proposed field-weakening methods based on voltage control enable maximum-torque operation both in IM and PMSM drives equipped with an LC filter.

An inverter output filter does not significantly affect the control performance of a variable-speed AC drive. The proposed control methods are based on cascaded controllers. Two additional control loops are needed due to the LC filter as compared to a drive without a filter. To ensure an adequate bandwidth separation between the control loops, the bandwidth of the stator current controller is about one third of that when a filter is not used. The speed control performance is close to that of a drive without a filter.

When using a sinusoidal CM filter at the inverter output, the modulation method should be selected carefully. The two-phase (or discontinuous) modulation method generates high lower-order harmonics in the CM voltage, which may excite the CM filter resonance and cause excessive oscillation in the CM current. Symmetrical suboscillation (or the corresponding space vector PWM) is suitable modulation method for drives equipped with a sinusoidal CM filter. The starting problem originating from the saturated CM inductor can be solved by modifying the on-durations of the zero vectors at the modulation start.

A cost-effective filter design requires knowledge of the component prices, motor and inverter parameters, and filtering requirements. In addition, the vector control sets a constraint for the filter design: the sampling frequency of the inverter output current should be at least four times the resonance frequency of the system. This requirement can be a limiting factor especially if the sampling frequency is low. Otherwise, the dominant requirement may be the THD of the stator voltage or the voltage drop in the filter inductor. Increasing the switching frequency of the inverter, the filter cost reduces, but on the other hand, the inverter power stage cost increases. An optimum switching frequency can be found if the inverter power stage cost is taken into account in the filter design.

Topics for future research could include the development of control methods that increase the bandwidth of the stator current control. If the cascaded controllers are replaced by some other control structure, the bandwidth of the stator current control could be closer to that of a drive without a filter. Speed-sensorless operation of IM drives equipped with an LC filter might be improved at low speeds if a signal injection method is applied. The development of identification methods for filter and motor parameters would be useful if the control methods presented in this thesis are to be implemented in commercial drives.

Bibliography

Akagi, H., Hasegawa, H., and Doumoto, T. (2004). "Design and performance of a passive EMI filter for use with a voltage-source PWM inverter having sinusoidal output voltage and zero common-mode voltage." *IEEE Trans. Power Electron.*, **19**(4), pp. 1069–1076.

Batzel, T. D. and Lee, K. Y. (2005). "Electric propulsion with sensorless permanent magnet synchronous motor: implementation and performance." *IEEE Trans. Energy Convers.*, **20**(3), pp. 575–583.

Belmans, R. M., D'Hondt, L., Vendenput, A. J., and Geysen, W. (1987). "Analysis of the audible noise of three-phase squirrel-cage induction motors supplied by inverters." *IEEE Trans. Ind. Appl.*, **23**(5), pp. 842–847.

Cacciato, M., Consoli, A., Scarcella, G., and Testa, A. (1999). "Reduction of common-mode currents in PWM inverter motor drives." *IEEE Trans. Ind. Appl.*, **35**(2), pp. 469–476.

Carpita, M., Colombo, D., and Monti, A. (2001a). "Innovative observer algorithm for sensorless control of ac permanent magnet synchronous machines." In *Proc. IEEE APEC'01*, pp. 865–871, Anaheim, CA.

Carpita, M., Colombo, D., Monti, A., and Fradilli, A. (2001b). "Power converter filtering techniques design for very high speed drive systems." In *Proc. EPE'01*, Graz, Austria.

Chen, S., Lipo, T. A., and Fitzgerald, D. (1995). "Measurement and analysis of induction motor bearing currents in PWM inverter drives." In *Proc. ACEMP'95*, pp. 289–296, Kusadasi, Turkey.

Chen, S., Lipo, T. A., and Novotny, D. W. (1996). "Circulating type motor bearing current in inverter drives." In *Conf. Rec. IEEE-IAS Annu. Meeting*, vol. 1, pp. 162–167, San Diego, CA.

Chen, X., Xu, D., Liu, F., and Zhang, J. (2007). "A novel inverter-output passive filter for reducing both differential- and common-mode dv/dt at the motor terminals in PWM drive systems." *IEEE Trans. Ind. Electron.*, **54**(1), pp. 419–426.

Choi, J.-W. and Sul, S.-K. (1995). "A new compensation strategy reducing voltage/current distortion in PWM VSI systems operating with low output voltages." *IEEE Trans. Ind. Appl.*, **31**(5), pp. 1001–1008.

Corley, M. J. and Lorenz, R. D. (1998). "Rotor position and velocity estimation for a salient-pole permanent magnet synchronous machine at standstill and high speeds." *IEEE Trans. Ind. Appl.*, **34**(4), pp. 784–789.

de Almeida, A. T., Ferreira, F., and Both, D. (2005). "Technical and economical considerations in the application of variable-speed drives with electric motor systems." *IEEE Trans. Ind. Appl.*, **41**(1), pp. 188–199.

Depenbrock, M. (1977). "Pulse width control of a 3-phase inverter with nonsinusoidal phase voltages." In *Proc. IEEE ISPC'77*, pp. 399–403.

Eskola, M. (2006). *Speed and position sensorless control of permanent magnet synchronous motors in matrix converter and voltage source converter applications*. Ph.D. thesis, Tampere Univ. Tech., Tampere, Finland.

Finlayson, P. T. (1998). "Output filters for PWM drives with induction motors." *IEEE Ind. Applicat. Mag.*, **4**(1), pp. 46–52.

Green, T. C., Hernandez-Aramburo, C. A., and Smith, A. C. (2003). "Losses in grid and inverter supplied induction machine drives." *IEE Proc.-Electr. Power Appl.*, **150**(6), pp. 712–724.

Hanigovszki, N. (2005). *EMC output filters for adjustable speed drives*. Ph.D. thesis, Inst. Energy Techn., Aalborg Univ., Aalborg, Denmark.

Hanigovszki, N., Poulsen, J., and Blaabjerg, F. (2003). "Performance comparison of different output filter topologies for ASD." In *Proc. EPE'03*, Toulouse, France.

Hanigovszki, N., Poulsen, J., and Blaabjerg, F. (2004). "A novel output filter topology to reduce motor overvoltage." *IEEE Trans. Ind. Appl.*, **40**(3), pp. 845–852.

Harnefors, L., Pietiläinen, K., and Gertmar, L. (2001). "Torque-maximizing field-weakening control: design, analysis, and parameter selection." *IEEE Trans. Ind. Electron.*, **48**(1), pp. 161–168.

Hava, A. M. (1998). *Carrier based PWM-VSI drives in the overmodulation region*. Ph.D. thesis, Univ. of Wisconsin-Madison, Madison, WI, USA.

Hinkkanen, M. (2004a). "Analysis and design of full-order flux observers for sensorless induction motors." *IEEE Trans. Ind. Electron.*, **51**(5), pp. 1033–1040.

Hinkkanen, M. (2004b). *Flux estimators for speed-sensorless induction motor drives*. Ph.D. thesis, Dept. Elect. Commun. Eng., Helsinki Univ. Tech., Espoo, Finland.

Hinkkanen, M. and Luomi, J. (2004). "Stabilization of regenerating-mode operation in sensorless induction motor drives by full-order flux observer design." *IEEE Trans. Ind. Electron.*, **51**(6), pp. 1318–1328.

Holtz, J. (2002). "Sensorless control of induction motor drives." *Proc. IEEE*, **90**(8), pp. 1359–1394.

Houldsworth, J. A. and Grant, D. A. (1984). "Use of harmonic distortion to increase the output voltage of a three-phase PWM inverter." *IEEE Trans. Ind. Appl.*, **20**(5), pp. 1224–1228.

Jalili, K., Malinowski, M., and Bernet, S. (2005). "Rotor flux oriented control of a high speed induction motor drive applying a two-level voltage source converter with LC-sine filter." In *Proc. EPE'05*, Dresden, Germany.

Kim, J.-M. and Sul, S.-K. (1997a). “Speed control of interior permanent magnet synchronous motor drive for the flux weakening operation.” *IEEE Trans. Ind. Appl.*, **33**(1), pp. 43–48.

Kim, J.-S. and Sul, S.-K. (1997b). “New approach for high-performance PMSM drives without rotational position sensors.” *IEEE Trans. Power Electron.*, **12**(5), pp. 904–911.

Kim, S.-H. and Sul, S.-K. (1997c). “Voltage control strategy for maximum torque operation of an induction machine in the field-weakening region.” *IEEE Trans. Ind. Electron.*, **44**(4), pp. 512–518.

Kim, S.-J. and Sul, S.-K. (1997d). “A novel filter design for suppression of high voltage gradient in voltage-fed PWM inverter.” In *Proc. IEEE APEC’97*, vol. 1, pp. 122–127, Atlanta, GA.

King, K. G. (1974). “A three phase transistor class-b inverter with sinewave output and high efficiency.” In *Inst. Elec. Eng. Conf. Publ. 123*, pp. 204–209.

Kojima, M., Hirabayashi, K., Kawabata, Y., Ejiogu, E. C., and Kawabata, T. (2004). “Novel vector control system using deadbeat-controlled PWM inverter with output LC filter.” *IEEE Trans. Ind. Appl.*, **40**(1), pp. 162–169.

Kolar, J. W., Ertl, H., and Zach, F. C. (1991). “Influence of the modulation method on the conduction and switching losses of a PWM converter system.” *IEEE Trans. Ind. Appl.*, **27**(6), pp. 1063–1075.

Kovács, K. P. and Rácz, I. (1959). *Transiente Vorgänge in Wechselstrommaschinen, Band I*. Verlag der Ungarischen Akademie der Wissenschaften, Budapest, Hungary.

Kubota, H., Matsuse, K., and Nakano, T. (1993). “DSP-based speed adaptive flux observer of induction motor.” *IEEE Trans. Ind. Appl.*, **29**(2), pp. 344–348.

Lai, Y.-S. (1999). “Investigations into the effects of PWM techniques on common mode voltage for inverter-controlled induction motor drives.” In *Proc. IEEE PES Winter Meeting*, vol. 1, pp. 35–40, New York, NY.

Lai, Y.-S. and Shyu, F.-S. (2004). “Optimal common-mode voltage reduction PWM technique for inverter control with consideration of the dead-time effects—Part I: Basic development.” *IEEE Trans. Ind. Appl.*, **40**(6), pp. 1605–1612.

Maes, J. and Melkebeek, J. A. (2000). “Speed-sensorless direct torque control of induction motors using an adaptive flux observer.” *IEEE Trans. Ind. Appl.*, **36**(3), pp. 778–785.

Mäki-Ontto, P. (2006). *Modeling and reduction of shaft voltages in AC motors fed by frequency converters*. Ph.D. thesis, Dept. Elect. Commun. Eng., Helsinki Univ. Tech., Espoo, Finland.

Mohan, N., Undeland, T. M., and Robbins, W. P. (1995). *Power Electronics: Converters, Applications, and Design*. John Wiley & Sons, New York, NY, 2nd edn.

Muetze, A. (2005). “Scaling issues for common mode chokes to mitigate ground currents in inverter-based drive systems.” In *Conf. Rec. IEEE-IAS Annu. Meeting*, vol. 3, pp. 1860–1867, Hong Kong, China.

Muetze, A. and Binder, A. (2005). “Systematic approach to bearing current evaluation in variable speed drive systems.” *Eur. Trans. Elect. Power*, **15**(3), pp. 217–227.

Murai, Y., Kubota, T., and Kawase, Y. (1992a). “Leakage current reduction for a high-frequency carrier inverter feeding an induction motor.” *IEEE Trans. Ind. Appl.*, **28**(4), pp. 858–863.

Murai, Y., Riyanto, A., Nakamura, H., and Matsui, K. (1992b). “PWM strategy for high frequency carrier inverters eliminating current-clamps during switching dead-time.” In *Conf. Rec. IEEE-IAS Annu. Meeting*, pp. 317–322, Houston, TX.

Murai, Y., Watanabe, T., and Iwasaki, H. (1987). “Waveform distortion and correction circuit for PWM inverters with switching lag-times.” *IEEE Trans. Ind. Appl.*, **IA-23**(5), pp. 881–886.

Nabae, A., Kitamura, M., Okamura, Y., and Peng, F. (1992). “A novel inverter with sinusoidal voltage and current output.” In *Conf. Rec. IEEE-IAS Annu. Meeting*, vol. 1, pp. 867–871, Houston, TX.

Nabae, A., Nakano, H., and Okamura, Y. (1994). “A novel control strategy of the inverter with sinusoidal voltage and current outputs.” In *Proc. IEEE PESC’94*, vol. 1, pp. 154–159, Taipei, Taiwan.

Ogasawara, S. and Akagi, H. (1996). “Modeling and damping of high-frequency leakage currents in PWM inverter-fed AC motor drive systems.” *IEEE Trans. Ind. Appl.*, **32**(5), pp. 1105–1114.

Ogasawara, S., Akagi, H., and Nabae, A. (1989). “A novel PWM scheme of voltage source inverter based on space vector theory.” In *Proc. EPE’89*, vol. 1, pp. 1197–1202, Aachen, Germany.

Ollila, J., Hammar, T., Iisakkala, J., and Tuusa, H. (1997). “On the bearing currents in medium power variable speed AC drives.” In *Proc. IEEE IEMDC’97*, Milwaukee, WI.

Palma, L. and Enjeti, P. (2002). “An inverter output filter to mitigate dV/dt effects in PWM drive system.” In *Proc. IEEE APEC’02*, vol. 1, pp. 550–556, Dallas, TX.

Park, J.-D., Khalizadeh, C., and Hofmann, H. (2005). “Design and control of high-speed solid-rotor synchronous reluctance drive with three-phase LC filter.” In *Conf. Rec. IEEE-IAS Annu. Meeting*, pp. 715–722, Hong Kong, China.

Pedersen, J. K., Blaabjerg, F., Jensen, J. W., and Thøgersen, P. (1993). “An ideal PWM-VSI inverter with feedforward and feedback compensation.” In *Proc. EPE’93*, vol. 4, pp. 312–318, Brighton, U.K.

Persson, E. (1992). “Transient effects in application of PWM inverters to induction motors.” *IEEE Trans. Ind. Appl.*, **28**(5), pp. 1095–1101.

Petkovšek, M., Zajec, P., and Nastran, J. (2000). “Magnetizing rotor flux determination using a time-discrete voltage source inverter.” In *Proc. MELECON 2000*, Nicosia, Cyprus.

Piippo, A. and Luomi, J. (2005). “Adaptive observer combined with HF signal injection for sensorless control of PMSM drives.” In *Proc. IEEE IEMDC’05*, pp. 674–681, San Antonio, TX.

Rapp, H. and Haag, J. (1997). “Stator current control for high-speed induction machines operated from inverters with LC-output-filter.” *European Transactions on Electrical Power*, **7**(4), pp. 235–242.

Rendusara, D. A. and Enjeti, P. N. (1998). “An improved inverter output filter configuration reduces common and differential modes dv/dt at the motor terminals in PWM drive systems.” *IEEE Trans. Power Electron.*, **13**(6), pp. 1135–1143.

Salomäki, J., Hinkkanen, M., and Luomi, J. (2005a). “Sensorless control of induction motor drives equipped with inverter output filter.” In *Proc. IEEE IEMDC’05*, pp. 332–339, San Antonio, TX.

Salomäki, J., Hinkkanen, M., and Luomi, J. (2005b). “Sensorless vector control of an induction motor fed by a PWM inverter through an output LC filter.” In *Proc. IPEC-Niigata 2005*, pp. 404–411, Niigata, Japan, CD-ROM.

Salomäki, J., Hinkkanen, M., and Luomi, J. (2007). “Influence of inverter output filter on maximum torque and speed of PMSM drives.” In *Proc. PCC Nagoya 2007*, pp. 852–859, Nagoya, Japan.

Salomäki, J. and Luomi, J. (2004). “Vector control of an induction motor fed by a PWM inverter with output LC filter.” In *Proc. NORPIE/2004*, Trondheim, Norway, CD-ROM.

Schauder, C. (1992). “Adaptive speed identification for vector control of induction motors without rotational transducers.” *IEEE Trans. Ind. Appl.*, **28**(5), pp. 1054–1061.

Schönung, A. and Stemmler, H. (1964). “Static frequency changers with “subharmonic” control in conjunction with reversible variable-speed a.c. drives.” *Brown Boveri Rev.*, **51**(8/9), pp. 555–577.

Seguier, G. and Labrique, F. (1993). *Power Electronic Converters: DC-AC Conversion*. Springer-Verlag, Berlin, Germany.

Sepe, R. B. and Lang, J. H. (1994). “Inverter nonlinearities and discrete-time vector current control.” *IEEE Trans. Ind. Appl.*, **30**(1), pp. 62–70.

Slemon, G. R. (1989). “Modelling of induction machines for electric drives.” *IEEE Trans. Ind. Appl.*, **25**(6), pp. 1126–1131.

Sozer, Y., Torrey, D. A., and Reva, S. (2000). “New inverter output filter topology for PWM motor drives.” *IEEE Trans. Power Electron.*, **15**(6), pp. 1007–1017.

Suwankawin, S. and Sangwongwanich, S. (2002). “A speed-sensorless IM drive with decoupling control and stability analysis of speed estimation.” *IEEE Trans. Ind. Electron.*, **49**(2), pp. 444–455.

Svensson, T. (1988). *On modulation and control of electronic power convertors*. Ph.D. thesis, Chalmers Univ. of Tech., Gothenburg, Sweden.

Swamy, M. M., Yamada, K., and Kume, T. (2001). “Common mode current attenuation techniques for use with PWM drives.” *IEEE Trans. Power Electron.*, **16**(2), pp. 248–255.

Szczupak, P. and Pacas, M. (2006). “Automatic identification of a PMSM drive equipped with an output LC-filter.” In *Proc. IEEE IECON’06*, pp. 1143–1148, Paris, France.

Teodorescu, R., Bech, M., Blaabjerg, F., and Pedersen, J. K. (2000). “Flexible drive systems laboratory – a modern teaching facility in electrical drives at Aalborg University.” In *Proc. NORPIE/2000*, pp. 42–26, Aalborg, Denmark.

van der Broeck, H. and Loef, C. (1995). “Use of LC filters in hard switching PWM inverter drives.” In *Proc. EPE’95*, Sevilla, Spain.

van der Broeck, H. W., Skudelny, H.-C., and Stanke, G. V. (1988). “Analysis and realization of a pulsewidth modulator based on voltage space vectors.” *IEEE Trans. Ind. Appl.*, **24**(1), pp. 142–150.

von Jouanne, A., Enjeti, P., and Gray, W. (1995). “The effect of long motor leads on PWM inverter fed AC motor drive systems.” In *Proc. IEEE APEC’95*, vol. 2, pp. 592–597, Dallas, TX.

von Jouanne, A. and Enjeti, P. N. (1997). “Design considerations for an inverter output filter to mitigate the effects of long motor leads in ASD applications.” *IEEE Trans. Ind. Appl.*, **33**(5), pp. 1138–1145.

von Jouanne, A., Zhang, H., and Wallace, A. K. (1998). “An evaluation of mitigation techniques for bearing currents, EMI and overvoltages in ASD applications.” *IEEE Trans. Ind. Appl.*, **34**(5), pp. 1113–1122.

Wheeler, P. and Grant, D. (1997). “Optimised input filter design and low-loss switching techniques for a practical matrix converter.” *IEE Proc.-Electr. Power Appl.*, **144**(1), pp. 53–60.

Xiyou, C., Bin, Y., and Yu, G. (2002). “The engineering design and the optimization of inverter output RLC filter in AC motor drive system.” In *Proc. IEEE IECON’02*, pp. 175–180, Sevilla, Spain.

Yamazaki, K. and Seto, Y. (2006). “Iron loss analysis of interior permanent-magnet synchronous motors-variation of main loss factors due to driving condition.” *IEEE Trans. Ind. Appl.*, **42**(4), pp. 1045–1052.

Yang, G. and Chin, T.-H. (1993). “Adaptive-speed identification scheme for a vector-controlled speed sensorless inverter-induction motor drive.” *IEEE Trans. Ind. Appl.*, **29**(4), pp. 820–825.

Yang, G., Tomioka, R., Nakano, M., and Chin, T.-H. (1993). “Position and speed sensorless control of brushless DC motor based on an adaptive observer.” *Trans. IEEJ*, **113-D**(5), pp. 579–586.

Zimmermann, W. (1988). “Feldorientiert geregelter Umrichterantrieb mit sinusförmigen Maschinenspannungen.” *etzArchiv*, **10**(8), pp. 259–266.

ISBN 978-951-22-9129-8
ISBN 978-951-22-9130-4 (PDF)
ISSN 1795-2239
ISSN 1795-4584 (PDF)